



UNIVERSIDADE DE
COIMBRA

Albina Bushmalyova

**COMBINED ANTITUMOR STRATEGIES
MEDIATED BY HYBRID POLYMERIC AND
LIPID-BASED NANOSYSTEMS TO
HEPATOCELLULAR CARCINOMA**

Dissertação no âmbito do Mestrado em Bioquímica orientada pelo
Doutor Henrique Manuel dos Santos Faneca e Doutora Paula Cristina
Veríssimo Pires e apresentada ao Departamento de Ciências da Vida da
Universidade de Coimbra.

Fevereiro de 2022

Departamento de Ciências da Vida da Faculdade de Ciências e Tecnologias
da Universidade de Coimbra

COMBINED ANTITUMOR STRATEGIES MEDIATED BY HYBRID POLYMERIC AND LIPID-BASED NANOSYSTEMS TO HEPATOCELLULAR CARCINOMA

Albina Bushmalyova

Dissertação no âmbito do Mestrado em Bioquímica orientada pelo Doutor Henrique Manuel dos Santos Faneca e Doutora Paula Cristina Veríssimo Pires e apresentada ao Departamento de Ciências da Vida da Universidade de Coimbra.

Fevereiro de 2022



UNIVERSIDADE DE
COIMBRA

Agradecimientos/Acknowledgements

Agradecimentos/Acknowledgments

Após dois anos desafiantes e incrivelmente interessantes, está na hora de agradecer a todos aqueles que de alguma maneira fizeram parte deste trajeto tão importante! Fazer um caminho com alguém ao nosso lado torna-se menos aborrecido e difícil, torna-se mais cativante e o objetivo traçado torna-se menos distante. A todos os que caminharam comigo neste percurso expresso o meu agradecimento:

Ao Dr. Henrique Manuel dos Santos Faneca por ter fortalecido o gosto pela nanotecnologia e por me ter aceitado no seu grupo de investigação para a realização da minha dissertação. Agradeço a sua sabedoria, conhecimento e experiência partilhada, por estar sempre presente e atento ao meu trabalho e, claro, ao seu esforço em ajudar e orientar da melhor maneira possível o meu projeto.

À Dina que, independentemente, dos meus “atrasos cerebrais” foi sempre compreensível e nunca desistiu de mim. Agradeço imenso a sua ajuda, apoio e participação na minha dissertação. Aos cafés e conversas partilhadas durante este percurso, que teria sido muito mais complicado sem estes pormenores. É com grande contentamento que digo, que durante este ano a Dina se tornou minha amiga e não apenas colega!

Agradeço a todos os membros do grupo de investigação HF, a todos os colegas de laboratório com os quais trabalhei durante este ano, a todos os professores, funcionários da Universidade de Coimbra e colegas académicos pela ajuda prestada quando mais precisava e pelo conhecimento passado.

Aos meus amigos Alfaiate, Andreia, Ana Raquel, Diana, Fernando, Mariana, Monteiro e Renata, por ouvirem os meus desabafos e preocupações, sejam estes relacionadas com a vida académica ou com outro assunto pessoal. Por demonstrarem interesse nas minhas “descobertas científicas”, pelo apoio e grande ajuda prestada, e claro, pelos bons momentos passados.

Ao meu irmão e à Dana, por serem o meu refúgio, pelo seu apoio, por me ajudarem a levantar a minha autoestima quando esta está em baixo e por todas as aventuras vividas e ainda por viver.

Ao Daniel, pelo seu apoio, presença e compreensão nesta última fase igualmente importante e difícil, pelo interesse demonstrado, a sua atenção e auxílio e por todos os momentos partilhados.

E finalmente, aqueles sem os quais nada disto seria possível, aos meus PAIS! Agradeço todo o apoio que me foi dado durante toda a minha vida, pela paciência e força, pelas conversas de adultos e exemplo impecável! Agradeço a ajuda que me prestaram nos obstáculos que foram aparecendo durante o caminho, pela preocupação constante e pelo amor que sempre foi demonstrado! É indiscutível que, no meu mundo, vocês são os melhores pais do mundo! Дуже дякую, все це завдяки вам! Я вас дуже люблю! Ви в мене самі найкращі!

Table of contents

Table of contents

List of abbreviations.....	v
Abstract.....	viii
Resumo.....	xii
1. INTRODUCTION.....	1
1.1. Hepatocellular carcinoma.....	2
1.1.1. Available treatment.....	3
1.2. Major HCC receptors and molecular signaling pathways.....	4
1.3. Selected drugs for the new therapeutic strategy against hepatocellular carcinoma.....	6
1.3.1. Afatinib.....	6
1.3.2. BMS-777607.....	7
1.3.3. XAV-939.....	7
1.4. Asialoglycoprotein receptor and ligands.....	8
1.5. Nanotechnology and nanosystems.....	9
1.5.1. PLGA nanoparticles and liposomes.....	11
1.5.2. Hybrid nanosystems.....	12
1.5.3. Nanosystem formulation for this project.....	14
1.6. Objective.....	15
2. MATERIALS AND METHODS.....	16
2.1. Materials.....	17
2.2. Methods.....	18
2.2.1. Hybrid nanosystem production and drug encapsulation.....	18
2.2.1.1. PLGA nanoparticle production.....	19
2.2.1.2. Liposome production.....	20
2.2.1.3. Hybrid nanosystems production.....	21
2.2.2. Characterization of nanoparticles.....	21
2.2.3. Cell culture.....	22
2.2.4. Cell viability.....	22
2.2.5. Cellular uptake and internalization of the nanoparticles.....	23
2.2.6. Cellular death mechanisms (apoptosis or necrosis).....	23
3. RESULTS.....	25
3.1. Incubation of HCC cell lines with different combinations of free drugs.....	26
3.1.1. Afatinib and XAV-939 combination in HepG2, Hep3B and Huh7 cells.....	26
3.1.2. BMS-777607 and Afatinib combination in HepG2, Hep3B and Huh7 cells.....	29
3.1.3. BMS-777607 and XAV-939 combination in HepG2, Hep3B and Huh7 cells.....	31
3.1.4 BMS-777607 afatinib and XAV-939 combination in HepG2, Hep3B and Huh7 cells.....	33
3.2. Apoptosis/Necrosis of HCC cells treated with the combination of free drugs.....	35

3.3. Production of hybrid nanosystems.....	39
3.3.1. Optimization of the PLGA nanoparticles using a sonication probe.....	39
3.3.2. Production of hybrid nanoparticles, encapsulation of the drugs, and evaluation of their therapeutic potential.....	40
3.4. Production of Asialofetuin-coated PLGA nanoparticles loaded with BMS-777607 and evaluation of their therapeutic potential.....	45
3.5. Production of liposomes loaded with afatinib, BMS-777607 and XAV-939 drugs, and evaluation of their therapeutic potential.....	50
4. DISCUSSION.....	54
4.1. Effect of different drug combinations in HCC cell lines.....	55
4.1.2. Apoptosis/Necrosis of HCC cells treated with the different drug combinations.....	56
4.2. Production of hybrid nanosystems and encapsulation of the drugs.....	57
4.3. Production of Asialofetuin-coated PLGA nanoparticles loaded with BMS-777607.....	59
4.4. Production of liposomes loaded with afatinib, BMS-777607 and XAV-939.....	61
5. CONCLUSION.....	62
6. REFERENCES.....	65

List of abbreviations

List of abbreviations

AFB1 – Aflatoxin B1

ASF – Asialofetuin

ASGP – Asialoglycoprotein

ATP – Adenosine triphosphate

Ca²⁺ - Calcium

Chol – Cholesterol

DLS – Dynamic light scattering

DMEM - Dulbecco's modified Eagle's medium

DMAB - didecyldimethylammonium bromide

DMSO - Dimethyl sulfoxide

DNA – Deoxyribonucleic acid

DSPE-PEG2000 - 1,2-distearoyl-sn-glycero-3-phosphoethanolamine- N-[amino(polyethylene glycol)-2000]

EGFR - epidermal growth factor receptor

EPR effect – Enhanced permeability and retention effect

FBS - Fetal bovine serum

FDA – Food and Drug Administration

GA- glycolic acid

GalNAc - N-acetylgalactose-amine

HBV – Hepatitis B Virus

HCC – Hepatocellular carcinoma

HCV – Hepatitis C Virus

HGF receptor - Hepatocyte growth factor receptor

HIF - hypoxia-inducible factors

HNSCC – Head and neck squamous cell carcinoma

LA- Lactic acid

LPNs – Lipid-polymer hybrid nanosystems

MDR – Multidrug resistance

NAFLD – Non-alcoholic fatty liver disease

NP - Nanoparticle

NSCLC - non-small-cell lung carcinoma

PI – Propidium Iodide

PLGA - Poly(D,L-lactic-co-glycolic acid)

POPC - 1-palmitoyl-2-oleoyl-sn-glycero -3-phosphocholine

PS – Phosphatidyl serine

VEGF - Vascular Endothelial growth factor

Abstract

Abstract

Hepatocellular carcinoma (HCC) is a liver malignancy that has high rates of morbidity and mortality, being the leading cause of mortality in the world associated to cancer. HCC is often diagnosed in late stages of its development, due to the lack of symptoms and effective screening strategies, stages in which an effective treatment is hard to achieve.

Currently there are some available treatment options to HCC. Sadly, these options are not effective enough when the HCC stages of development are advanced, therefore, only a small percentage of individuals who suffer from this disease can, in fact, receive an effective treatment. As a result of this limitation, systemic chemotherapy with cytotoxic agents is often applied to the patients, showing only a slight improvement. Given this, it is an urgent matter to develop new antitumor approaches with high rates of HCC targeting and treatment effectiveness.

During hepatocarcinogenesis various molecular signaling pathways are dysregulated, giving rise to favourable cellular processes in HCC development. Their study might provide novel therapeutic strategies against hepatocellular carcinoma. Drugs like afatinib (BIBW2992), BMS-777607 (BMS 817378) and XAV-939 (NVP-XAV939) have the ability to inhibit some of these overexpressed or overactivated molecular targets (EGFR, c-MET and Wnt/ β catenin respectively) and, consequently, could attenuate the HCC progression and have an effective antitumor effect. Unfortunately, using these drugs without a delivery system, most likely, will result in a limited therapeutic effect and will cause negative side effects, since its delivery will not be a specific one, not targeted to the HCC cells.

Recently, our group developed a hybrid nanosystem formulation that have the ability to efficiently and specifically deliver drugs to the HCC cells. Its specificity is due to the presence of the GalNAc ligand that specifically binds to the ASGP (asialoglycoprotein) receptors that are overexpressed in the HCC cells surface. In this context, the main goals of this project were to develop an effective antitumor strategy to HCC, through afatinib, BMS-777607 and XAV-939 drug combinations, and decrease possible side effects, reducing cytotoxicity to non-tumor cells, through drug encapsulation in specific nanosystems to HCC cells.

In this work several studies have been performed in order to analyse whether the combination of afatinib, BMS-777607 and XAV-939 has a synergistic antitumor effect and whether their encapsulation in nanosystems constitutes an effective therapeutic approach against hepatocellular carcinoma. Hepatocellular carcinoma cells (HepG2, Hep3B and Huh7 cells) were incubated with different combinations of free drugs and their synergistic effect was evaluated. Apoptosis/necrosis levels were evaluated in order to analyse the cellular death mechanisms involved in the therapeutic effect promoted by the drugs. Afterwards, the drug combinations with higher potential were encapsulated in hybrid nanosystems, in PLGA nanoparticles or in liposomes

and loading capacity and efficiency of the different nanocarriers were determined. Asialofetuin (ASF), another specific ligand of the ASGP receptors, was attached to the PLGA nanoparticles, as an alternative to the GalNAc ligand present in the liposomes, in order to maintain the specificity to HCC cells. Then, the cellular uptake and internalization of these PLGA nanoparticles and liposomes were analysed in the HCC cells. Moreover, the cytotoxicity of the individual and combined free drugs and of those drugs encapsulated in the different nanocarriers was evaluated in HCC cells.

The obtained results relatively to the assays performed with free drugs showed that some combinations possess synergistic effect when used in pairs or the three altogether, meaning that the new drug combinations are able to produce an effective antitumor effect against the HCC cells. This synergy was demonstrated by apoptosis/necrosis assays, that confirmed cellular death, which occurred mostly by apoptosis. Posterior encapsulation of the drugs in hybrid nanosystems brought some challenges, given that afatinib and XAV-939 drugs presented low percentages of encapsulation in PLGA nanoparticles. Thus, these drugs were consequently encapsulated in the liposomes while BMS-777607 was encapsulated in PLGA nanoparticles. The mixture of liposomes encapsulating afatinib and XAV-939 and PLGA nanoparticles encapsulating BMS-777607 took place to create hybrid nanosystems. The cell viability levels of HCC cells after incubation with hybrid nanosystems encapsulating the drug combinations were high for most of the tested conditions, with the exception of HepG2 cells, incubated with the BMS 0.5 μ M/ AFT 0.5 μ M/ XAV 0.5 μ M drug combination, and the Hep3B cells, treated with the BMS 1 μ M/ AFT 0.25 μ M/ XAV 0.25 μ M combination, that presented a significant decrease of cell viability.

BMS-777607 drug was encapsulated in PLGA nanoparticles only coated with asialofetuin (ASF) to maintain nanoparticles specificity to HCC cells. Different ASF concentrations were tested in order to determine cellular internalization of the nanoparticles, and 125 μ g ASF/mg NP was chosen for further studies due to the high cell uptake registered. Cells were incubated with produced empty PLGA nanoparticles and nanoparticles encapsulating BMS-777607 drug, both coated with ASF or not. The obtained cell viability levels were substantially reduced after incubation with nanoparticles encapsulating the drug.

In order to take advantage of the synergistic effect that resulted from the combination of the drugs, liposomes were used to encapsulate the three drugs, afatinib, BMS-777607 and XAV-939. Cellular internalization was evaluated and, once again, a high cell uptake of the nanosystems by HCC cells was observed. Posteriorly, incubation of the cells with liposomes loaded with the drugs was carried out. Although, the cell viability levels were not significantly affected for most of the conditions, for Hep3B cells treated with the BMS 0.5 μ M/ AFT 0.5 μ M/ XAV 0.5 μ M and BMS 1 μ M/ AFT 0.25 μ M/ XAV 0.25 μ M drug combinations a significant cytotoxicity was observed.

Overall, the obtained results in this dissertation were promising, but further studies need to take place in order to achieve final answers to the proposed hypotheses. The combination of the free drugs Afatinib, BMS-777607 and XAV-939, resulted in an outstanding synergistic effect in inducing cellular death to HCC cells, even greater results were obtained when the three drugs were combined, although the two-by-two combinations also resulted in low cell viability percentages. When the drug or its combinations were encapsulated in nanosystems, hybrid nanosystems, PLGA nanoparticles and liposomes, in some cases it was possible to note that HCC cell viability percentages dropped, raising hope as to the therapeutic effect of the produced nanosystems. The antitumoral effect of the drugs to the HCC cells and the synergistic effect of their combination alongside with the nanosystem formulations could be a promising tool to treat hepatocellular carcinoma, improving the quality of life of the patients that suffer from this disease.

KEYWORDS: Hepatocellular carcinoma, hybrid nanosystems, molecular signaling pathways, therapeutic agents, synergistic effect.

Resumo

Resumo

O carcinoma hepatocelular (HCC) é uma doença maligna do fígado que apresenta taxas elevadas de morbidade e mortalidade, sendo atualmente a segunda causa de mortalidade no mundo associada ao cancro. O HCC é frequentemente diagnosticado em estádios avançados do seu desenvolvimento, devido à falta de sintomas e de estratégias de rastreio eficazes, sendo que nesses estádios é muito difícil obter um tratamento eficaz.

Atualmente, existem algumas opções de tratamento disponíveis para o HCC. Contudo, essas opções não são suficientemente eficazes quando os estádios de desenvolvimento do HCC estão numa fase avançada, portanto, apenas uma pequena percentagem de indivíduos que sofrem desta doença pode, de facto, receber um tratamento eficaz. Em decorrência dessa limitação, a quimioterapia sistémica com agentes citotóxicos é frequentemente aplicada aos pacientes, apresentando apenas uma ligeira melhoria. Neste contexto, é urgente desenvolver novas abordagens antitumorais que apresentem maior especificidade para HCC e maior eficácia.

Durante a hepatocarcinogénese várias vias de sinalização moleculares estão desreguladas, dando origem a processos celulares favoráveis ao desenvolvimento do HCC. O seu estudo poderá permitir o desenvolvimento de novas estratégias terapêuticas contra o carcinoma hepatocelular. Fármacos como afatinib, BMS-777607 e XAV-939 têm a capacidade de inibir alguns desses alvos moleculares sobreexpressos ou sobreativos no HCC (EGFR, c-MET e Wnt/ β catenina, respetivamente) e, conseqüentemente, podem atenuar a progressão do HCC e aumentar o efeito antitumoral. Contudo, a utilização desses fármacos sem um sistema de entrega irá resultar, possivelmente, num efeito terapêutico limitado e efeitos secundários negativos, uma vez que a sua entrega não será específica, isto é, direcionada para as células de HCC.

Recentemente, o nosso grupo desenvolveu uma formulação de nanossistema híbrido que tem a capacidade de entregar fármacos de forma eficiente e específica às células de HCC. A sua especificidade deve-se à presença do ligando GalNAc que se liga especificamente aos recetores de ASGP (asialoglicoproteína) que estão sobreexpressos na superfície das células de HCC. Neste contexto, os principais objetivos deste projeto foram desenvolver uma estratégia antitumoral eficaz para HCC, através da combinação dos fármacos afatinib, BMS-777607 e XAV-939, e diminuir possíveis efeitos secundários, reduzindo a citotoxicidade para as células não tumorais, através da encapsulação dos fármacos em nanossistemas específicos para células de HCC.

Nesta dissertação foram realizados vários estudos com o propósito de avaliar se a combinação dos fármacos afatinib, BMS-777607 e XAV-939 resulta um efeito sinérgico, e se a sua encapsulação em nanossistemas promove uma ação terapêutica eficaz contra o HCC. As células de carcinoma hepatocelular (HepG2, Hep3B e Huh7) foram incubadas com diferentes combinações dos fármacos livres, tendo sido avaliado o seu possível efeito sinérgico. Foram

realizados ensaios de apoptose/necrose para analisar os mecanismos de morte celular induzidos pelos fármacos. Posteriormente, as combinações de fármacos com maior potencial foram encapsuladas nos nanossistemas híbridos, em nanopartículas de PLGA e em lipossomas, tendo sido determinada a capacidade e a eficiência de carregamento das diferentes nanopartículas. A asialofetúina (ASF), outro excelente ligando para os recetores das ASGPs, foi associada às nanopartículas de PLGA, como alternativa ao ligando GalNAc presente nos lipossomas, com o objetivo de manter a especificidade para as células de HCC. Neste sentido, foi avaliada a internalização celular das nanopartículas de PLGA e dos lipossomas nestas células. Adicionalmente, foi avaliada a citotoxicidade dos fármacos livres, usados individualmente e em combinação, e dos fármacos encapsulados nas diferentes nanopartículas em células de HCC.

Os resultados obtidos com as novas combinações de fármacos, quando comparados com os obtidos com os fármacos livres, mostraram que algumas das combinações possuem um efeito sinérgico substancial, resultando numa ação antitumoral eficaz contra as células de HCC. A observação desta sinergia foi reforçada pelos resultados obtidos nos ensaios de apoptose/necrose, que confirmaram que a morte celular induzida por estas novas estratégias ocorreu principalmente por apoptose. O encapsulamento posterior dos fármacos em nanossistemas híbridos trouxe alguns desafios, visto que os fármacos afatinib e XAV-939 apresentaram baixas eficiências de encapsulação em nanopartículas de PLGA. Consequentemente, estes fármacos foram encapsulados nos lipossomas enquanto o BMS-777607 foi encapsulado nas nanopartículas de PLGA. Procedeu-se à mistura dos lipossomas que encapsularam afatinib e XAV-939 e de nanopartículas de PLGA que encapsularam BMS-777607 para criar nanossistemas híbridos. Os níveis de viabilidade celular registados após a incubação com os nanossistemas híbridos contendo os fármacos apresentaram-se elevados para as linhas celulares testadas, com exceção das células HepG2, para a combinação de fármacos BMS 0.5 μ M/ AFT 0.5 μ M/ XAV 0.5 μ M, e das células Hep3B, para a combinação BMS 1 μ M/ AFT 0.25 μ M/ XAV 0.25 μ M, que apresentaram uma diminuição significativa da viabilidade celular.

Numa abordagem diferente o fármaco BMS-777607 foi encapsulado em nanopartículas de PLGA apenas revestidas com asialofetúina (ASF), por forma a manter a especificidade das nanopartículas para as células de HCC. Foram testadas diferentes concentrações de ASF, para avaliar o seu efeito na internalização celular das nanopartículas, tendo sido escolhida a concentração de 125 μ g de ASF / mg de NP para estudos posteriores devido à elevada internalização celular registada. As células foram incubadas com nanopartículas PLGA vazias e nanopartículas carregadas com o fármaco BMS-777607, revestidas ou não com ASF. Os níveis de viabilidade celular registados foram substancialmente reduzidos após incubação com as nanopartículas carregadas com o fármaco.

Afim de tirar partido do efeito sinérgico resultante da combinação dos três fármacos, afatinib, BMS-777607 e XAV-939, estes foram encapsulados em lipossomas. Os ensaios de

internalização celular mostraram novamente a ocorrência de uma elevada internalização dos nanossistemas nas células de HCC. Posteriormente, as células foram incubadas com os lipossomas carregados com os fármacos, tendo-se verificado que os níveis de viabilidade celular não foram significativamente afetados na maioria das condições testadas, com exceção das células Hep3B tratadas com lipossomas contendo as combinações de fármacos BMS 0.5 μ M/ AFT 0.5 μ M/ XAV 0.5 μ M e BMS 1 μ M/ AFT 0.25 μ M/ XAV 0.25 μ M, onde se verificou uma citotoxicidade significativa.

De uma forma geral, alguns dos resultados obtidos nesta dissertação mostraram ser promissores, mas em alguns casos, estudos adicionais deverão ser realizados a fim de se obter respostas finais às hipóteses propostas. A combinação dos fármacos livres Afatinib, BMS-777607 e XAV-939, resultou num excelente efeito sinérgico no que toca a indução de morte celular das células de HCC, resultados ainda mais significativos foram obtidos quando os três fármacos foram combinados, embora as combinações dos mesmos dois a dois também resultou numa baixa percentagem de viabilidade celular. Quando os fármacos ou as suas combinações foram encapsulados em nanossistemas, nanossistemas híbridos, nanopartículas de PLGA e lipossomas, em alguns casos foi possível notar que as percentagens de viabilidade celular de HCC desceram, aumentando assim a esperança quanto ao efeito terapêutico dos nanossistemas produzidos. O efeito anti tumoral dos fármacos nas células de HCC e o efeito sinérgico das suas combinações juntamente com as formulações de nanossistemas podem ser uma ferramenta promissora para o tratamento do carcinoma hepatocelular, melhorando a qualidade de vida dos pacientes que sofrem desta doença.

PALAVRAS-CHAVE: Carcinoma hepatocelular, nanossistemas híbridos, vias de sinalização moleculares, agentes terapêuticos, efeito sinérgico.

1. Introduction

1. Introduction

1.1. Hepatocellular carcinoma

Cancer is the second leading cause of human death, it causes approximately 7.6 million deaths every year, which corresponds to 13% of total deaths worldwide. The number of people suffering from cancer are expected to rise in the future as well as cancer-related mortality (Chaturvedi *et al.*, 2018). During carcinogenesis an uncontrolled cell multiplication and the inhibition of the apoptotic processes occur. Cancer cells have the ability to invade other healthy parts of the human body through metastasis, compromising the functioning of vital organs in the organism (Azevedo *et al.*, 2021). Advances in medicine and investigation fields have been assisting in the treatment of cancer diseases and currently there are many therapeutic strategies that are available and successful. Nonetheless, the development of new techniques and approaches for precise diagnosis and treatment are still essential. To treat different types of cancers, chemotherapy and radiotherapy are treatments that are currently most used, but these present a great number of painful secondary effects that affect the patient's quality of life (Azevedo *et al.*, 2021; Zhang *et al.*, 2018).

Hepatocellular carcinoma (HCC) is the most common and prevalent liver malignancy, and it occurs as a consequence of the hepatic dysfunction and complex biological processes (Alqahtani *et al.*, 2019; Pinto Marques *et al.*, 2020). The percentage of occurrence of this pathology has been increasing through the years, having high rates of morbidity and mortality. Currently, HCC is the leading cause of death worldwide associated to cancer, with around 800.000 new diagnosed cases and 750.000 deaths every year. Due to the lack of symptoms and efficient screening strategies, around 80% of the patients are diagnosed with advanced HCC stages of development to which an effective treatment is no longer available (Dimri *et al.*, 2020). It is estimated that around 85% of HCC clinical cases occur in low-resource or middle-resource countries, located in Eastern Asia and sub-Saharan Africa, in which medical resources are sparse (Yang *et al.*, 2019).

There are many risk factors for the hepatocellular carcinoma development, these can be genetic or environmental, among them are chronic liver diseases or cirrhosis, the abuse in the alcohol consumption and/or tobacco, non-alcoholic fatty liver disease (NAFLD). Hepatitis B virus (HBV) and Hepatitis C virus (HCV) are responsible for the origin of 80% of HCC cases, therefore being the principal causes of HCC development. Aflatoxin, more precisely, Aflatoxin B1 (AFB1), a food contaminant, might be involved in the pathological processes of HCC, since

its consumption is able to trigger the HCC occurrence. Metabolic syndrome, such as obesity, diabetes, genetic and hereditary factors are also considered as risk factors for the HCC development as well as patient heterogeneity. Male individuals have a higher probability of HCC occurrence, presumably due to a higher prevalence of HBV and HCV and alcohol consumption in men, which can reflect into increased carcinogenesis (Alqahtani *et al.*, 2019; Fujiwara *et al.*, 2018; Hartke *et al.*, 2017; Jindal *et al.*, 2019; Kulik and El-Serag., 2019; Yang *et al.*, 2019).

1.1.1. Available treatments

Currently, there are some available treatment options to cure hepatocellular carcinoma or, at least, to reduce or delay its malignant effects. Surgical resection, radiofrequency/microwave ablation, trans arterial chemoembolization and liver transplantation are the curative treatments that can only be effective in early stages of HCC development (Alqahtani *et al.*, 2019). Once the tumour progress into advanced stages, medical assistance become sparse and not cost-effective, not to mention that in case of liver transplantation most of the time it is hard to find a suitable donor. Hence, an early diagnosis and prevention of the HCC development and progression becomes very important in patients at risk due to its health benefit (Alqahtani *et al.*, 2019; Fujiwara *et al.*, 2018).

Given the limitations of the effective treatment options, systemic chemotherapy is frequently applied to HCC patients, specially to those that the above-mentioned treatments are no longer an alternative. Sadly, hepatocellular carcinoma is resistant to conventional chemotherapy treatment with cytotoxic agents (Dimri *et al.*, 2020). Chemotherapy drugs slow down cancer cells from their rapid-growing through different strategies and action mechanisms, these could be by interfering with the cancer cells' DNA synthesis, its replication or transcription, and cell division (Azevedo *et al.*, 2021; Hossen *et al.*, 2018). Given this, only 30%-40% of patients with HCC have the chance to receive a proper treatment (Dimri *et al.*, 2020; Pinto Marques *et al.*, 2020).

Sorafenib is FDA approved drug and it is the first-line therapy for hepatocellular carcinoma treatment. Sorafenib is a multikinase inhibitor, that blocks VEGFR, PDGFR, c-KIT, RET receptors and Ras/Raf/MEK/ERK signaling pathway that are overexpressed in HCC carcinogenesis. Sorafenib is usually used in patients with advanced and intermediate-stage of HCC development (Dimri *et al.*, 2020; Farinha *et al.*, 2021). Although sorafenib exhibits a good antitumor activity in HCC, its clinical application is still limited due to its side effects and low targeting efficiency to the tumour. Furthermore, the long-term use of sorafenib lead to pERK up-regulation, giving rise to cellular resistance and consequently to tumour resistance and toxic reactions (Brunetti *et al.*, 2019; Farinha *et al.* 2021; Tang *et al.*, 2020; Zhang *et al.*, 2020).

1.2. Major HCC receptors and molecular signaling pathways

Hepatocellular carcinoma involves genetic and epigenetic alterations, such as mutations, deletions and abnormal gene expression, that occur in the oncogenes and/or tumour suppressor genes. During the hepatocarcinogenesis, several molecular signaling pathways are shown to possess abnormalities that intervene in the carcinogenic process of HCC (Figure 1). Its identification and study become very important since it might offer the development of a potential novel therapeutic strategy through the new identified targets (Dimri *et al.*, 2020). Several signaling pathways and receptors that are overexpressed, dysregulated or overactivated in HCC are already identified. These pathways contribute to HCC carcinogenesis development through the transcription of genes involved in hepatocellular carcinoma events (Dimri *et al.*, 2020; Whittaker *et al.*, 2010).

High expression of Vascular Endothelial growth factor (VEGF) and VEGF receptors have been detected in hepatocarcinoma cell lines, tissues and even in the serum of patients with HCC. This VEGF overexpression might be related to the hypoxic tumour environment, activation of EGF receptor and cyclo-oxygenase-2 signaling (Muto *et al.*, 2014). VEGF receptor acts on angiogenesis processes and is a regulatory factor in the carcinogenesis of hepatocellular carcinoma (Dimri *et al.*, 2020; Semela and Dufour., 2004). There are 3 subtypes of VEGF receptor and apparently the VEGFR-2 is the one that manages most of the cellular responses to VEGFs (Muto *et al.*, 2014). The induction of growth factors like hypoxia-inducible factors 1 and 2 (HIF 1 and 2) and insulin like growth factor 2 (IGF2) results from the severe hypoxia in HCC. Posteriorly, HIF1 and IGF2 activate the VEGF receptor, stimulating its expression as well as other growth factors, subsequently resulting in tumour angiogenesis, which in turn provokes tumour progression and metastases (Dimri *et al.*, 2020; Whittaker *et al.*, 2010).

Epidermal growth factor (EGF) receptor is often dysregulated in hepatocellular carcinoma. It is responsible for the regulation of several cellular processes in HCC that include proliferation, motility, angiogenesis and inhibition of the apoptosis. This signaling pathway is activated when the IGF-1 and IGF-2 ligands bind to the receptor (Alexia *et al.*, 2004). The binding provokes an auto-phosphorylation and activation of the receptor that is followed by phosphorylation of intracellular targets. In consequence, these processes result in the activation of PI3K/AKT/mTOR, MAPK, protein kinase B and RAF/MEK/ERK pathways. IGF-2 ligand is overexpressed in patients with HCC, this will result in its high binding to the receptor and consequently in an elevated receptor and signaling pathways activity (Dimri *et al.*, 2020; Wecker *et al.*, 2018; Whittaker *et al.*, 2010).

The hepatocyte growth factor receptor (HGFR) is a tyrosine receptor encoded by the c-MET proto-oncogene. It has been reported that c-MET might be involved in the development of various types of cancer. When c-MET/HGF receptor is activated, it contributes to tissue regeneration, cell proliferation, migration, survival, branch morphogenesis, and angiogenesis in hepatocellular carcinoma cells (Dimri *et al.*, 2020). The binding of the HGF ligand to the receptor leads to its phosphorylation and further phosphorylation of adaptor proteins, hence activating phospholipase C, PI3K and ERK signaling pathways (Dimri *et al.*, 2020; Matsumoto *et al.*, 1996; Whittaker *et al.*, 2010). Multiple molecular genetic factors are associated with c-MET dysregulation, and its overexpression leads to a reduced survival in HCC patients (Ueki *et al.*, 1997).

In WNT/ β -catenin signaling pathway, occurs an abnormal regulation of the β -catenin transcription factor, which is responsible for the development of the hepatocellular carcinoma early events (Apte *et al.*, 2007; Avila *et al.*, 2006). WNT ligands bind to the frizzled members of the WNT/ β -catenin signaling pathway receptor triggering the pathway's phosphorylation and posterior activation. Subsequently, the GSK3 β (glycogen synthase kinase 3 β) is inhibited, increasing the cytosolic β -catenin concentration. Consequently β -catenin is translocated to the nucleus and activates the transcription of genes involved in cell proliferation, angiogenesis, anti-apoptosis and the formation of extracellular matrix in HCC. An increase of β -catenin levels in the nucleus and cytoplasm have been observed in around 50-70% of tumors in HCC, thus an increased proliferation of tumor cells occurs. Given this, WNT plays an important role in the regulation of liver regeneration and self-renewal of pluripotent stem cells and progenitor cells, presenting itself as a promising target for HCC therapy (Dimri *et al.*, 2020; Whittaker *et al.*, 2010).

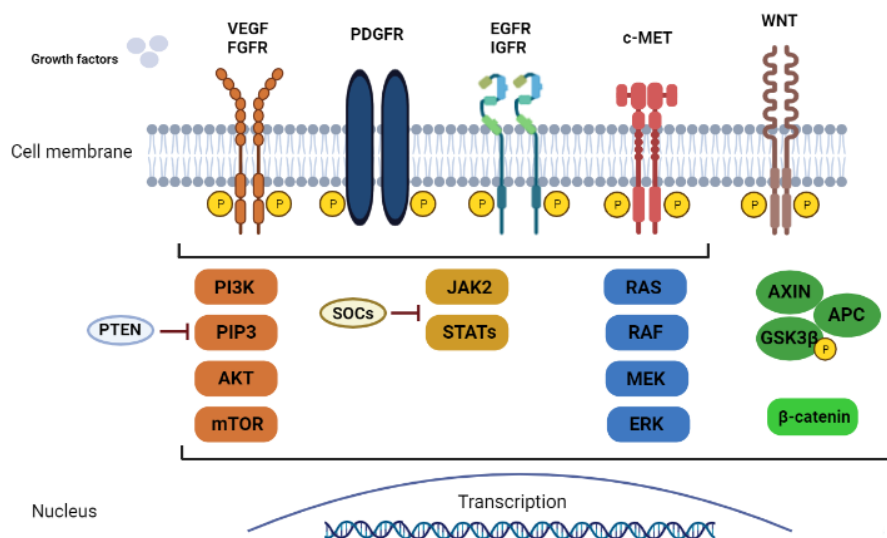


Figure 1. Major molecular signaling pathways involved in hepatocellular carcinoma (adapted from Dimri *et al.*, 2020).

1.3. Selected drugs for the new therapeutic strategy against hepatocellular carcinoma

Given the complexity of hard-to-treat diseases like cancers, monotherapy is evolving to combined therapies or multiple therapies, enhancing drug efficiencies and therapeutic effectiveness through synergy (Farinha *et al.*, 2021). In this context, the combination of the drugs afatinib, BMS-777607 and XAV-939, which are responsible for the inhibition of EGFR, c-MET and WNT/ β -catenin receptors, respectively, could result in an effective therapeutic approach. These drugs or its combination were not tested in HCC before, nevertheless the combination of the three drugs might result in a positive synergistic effect, thus increasing their therapeutic potential for HCC treatment.

1.3.1. Afatinib

Afatinib (BIBW 2992) is an adenosine triphosphate (ATP)-competitive anilino-quinazoline derivative containing a reactive acrylamide group and a selective inhibitor of the receptor tyrosine kinases that inhibits EGFR, also known as ErbB1, (IC₅₀ = 0.5 nM) that belong to the ErbB protein family (Ferraroto *et al.*, 2014; Wecker and Waller., 2018).

Afatinib activity is irreversible and possesses a multi-receptor binding. It binds to cysteine 797 of the EGFR, leading to reduced phosphorylation processes and consequent inhibition of the downstream pathways (Wecker and Waller., 2018). Generally, according to previous tests in different cell lines, afatinib has the ability to suppress the EGFR, ErbB2, ErbB3, ErbB4, HER2, ERK and AKT phosphorylations. As a result, apoptotic processes are activated reducing carcinogenesis and tumour growth (Ferraroto *et al.*, 2014; Li *et al.*, 2008; Wecker and Waller., 2018).

Overall, afatinib has already been tested as a treatment in various tumour types, like lung cancer, non-small-cell lung carcinoma (NSCLC), head and neck squamous cell carcinoma (HNSCC), breast cancer and brain metastases. A reduction in the tumour activity was detected in xenograft and transgenic lung cancer mouse models after afatinib administration (Ferrarotto *et al.*, 2014; Li *et al.*, 2008; Wecker and Waller., 2018), and in case of NSCLC patients, a significant improvement occurred following chemotherapy with gefitinib and erlotinib after afatinib administration (Harvey *et al.*, 2020).

1.3.2. BMS-777607

BMS-777607 (BMS 817378) is an ATP-competitive MET kinase inhibitor. It targets several MET family members that include c-MET receptor, also known as HGFR, RON, Axl and Tyro3. BMS-777607 provokes an inhibition of the c-MET receptor by inhibiting its autophosphorylation and consequent activation of the downstream molecular signaling pathways (Dai *et al.*, 2012; Wu *et al.*, 2019). BMS-777607 binds to the c-MET active site with an inhibitor constant (K_i) value of 3.9 nmol/L. According to pre-clinical models, it exhibited an effective blockage of c-MET autophosphorylation with an IC₅₀ of 20 nmol/L (Dai and Siemann., 2010). Moreover, it has been reported that BMS-777607 have the ability to block Mer, Flt-3, Aurora B, Lck and VEGF receptor 2 (Wu *et al.*, 2019).

According to available literature, BMS-777607 has already been used to treat diseases like breast cancer, ovarian cancer, prostate cancer and intra-hepatic cholangiocarcinoma. As to breast cancer, BMS-777607 showed its therapeutic effect through the inhibition of the RON receptor inducing breast cancer cell polyploidy (Sharma *et al.*, 2013). BMS-777607 activity has been used to inhibit HGF-independent c-MET auto-phosphorylation to suppress ovarian carcinogenesis activity (Wu *et al.*, 2019). It was reported that BMS-777607 inhibits HGF-induced prostate cancer cell scattering, and suppresses HGF-induced cell migration, cell invasion and cell proliferation (Dai and Siemann., 2010).

1.3.3. XAV-939

XAV-939 (NPV-XAV 939) is able to inhibit the WNT/ β -catenin signalling pathway by stabilising a scaffolding protein, AXIN. XAV-939 stabilises AXIN by inhibiting the poly-ADP-ribosylating enzymes tankyrase 1 and tankyrase 2. When WNT/ β -catenin pathway is active, an abnormal regulation of the transcription factor, β -catenin, occurred. AXIN anchors proteins that are involved in the degradation of the β -catenin complex; therefore, it is responsible for β -catenin degradation and inactivation of the WNT/ β -catenin signalling pathway (Dittfeld *et al.*, 2018; Huang *et al.*, 2009). According to literature, XAV-939 is mainly used to treat diseases like calcification of human valvular interstitial cells (Dittfeld *et al.*, 2018), it ameliorates osteoarthritis in murine model through Wnt/ β -catenin inhibition (Lietman *et al.*, 2018), and enhances osteoblastogenesis and mineralization of human skeletal stem cells (Almasoud *et al.*, 2020).

1.4. Asialoglycoprotein receptor and ligands

The asialoglycoprotein receptor (ASGPR) (Figure 2) is a highly conserved transmembrane heteromeric glycoprotein, first identified by Ashwell and Harford (Geffen and Spiess., 1993). It is a Ca^{2+} -dependent carbohydrate-binding protein, or C-type lectin. ASGPR is expressed by parenchymal cells of the liver (hepatocytes) and it is minimally present in other body tissues (Farinha *et al.*, 2021; Khorev *et al.*, 2008). The uptake of glycoproteins with terminal N-acetylgalactosamine (GalNAc) or galactose residues (asialoglycoproteins) by the liver cells is facilitated by ASGPR. During this process, ASGPR binds and internalizes the molecules with exposed galactose or N-acetylgalactosamine residues, following the degradation of the terminal sialic acid present in the glycoproteins by sialidase enzyme (Igdoura., 2017; Nair *et al.*, 2014).

The human ASGPR consists of two homologous subunits, H1 and H2, which form a non-covalent heterooligomeric complex with 2-5:1 ratio, respectively. Both are single-spanning membrane proteins with a calcium-dependent galactose/GalNAc recognition domain. (Igdoura., 2017; Khorev *et al.*, 2008; Stokmaier *et al.*, 2009). The expression of asialoglycoprotein receptors is located on the sinusoidal and basolateral membrane of hepatocytes, but it can also be present on the surface of the proliferating hepatocellular carcinoma cells. The presence of the ASGPR on the HCC cells may offer an advantage in the treatment of this malignancy (Trerè *et al.*, 1998).

As ASGPR recognizes and exhibits specificity for the terminal galactose and GalNAc residues of glycoproteins, this receptor and the asialoglycoproteins have the ability to bind with each other (Igdoura., 2017; Nair *et al.*, 2014). Therefore, ASGP receptors appear to be the key for the specific drug delivery, mediated by the nanosystems containing the GalNAc ligand, to the HCC cells.

Asialofetuin exhibits affinity to ASGPR, therefore it is also an excellent ligand to these receptors. It is a negatively charged 48kDa glycoprotein and it possesses three asparagine-linked triantennary complex carbohydrate chains with terminal N-acetylgalactosamine residues, which, as mentioned above, are recognized by the ASGP receptors overexpressed in the HCC cells (Farinha *et al.*, 2014; Bider and Spiess., 1998; Wu *et al.*, 1998). ASF is endocytosed by hepatocyte cells and studies have showed that receptor-mediated endocytosis enhances liposome-associated drug delivery into hepatocytes (Detampel *et al.*, 2014; Wu *et al.*, 1998).

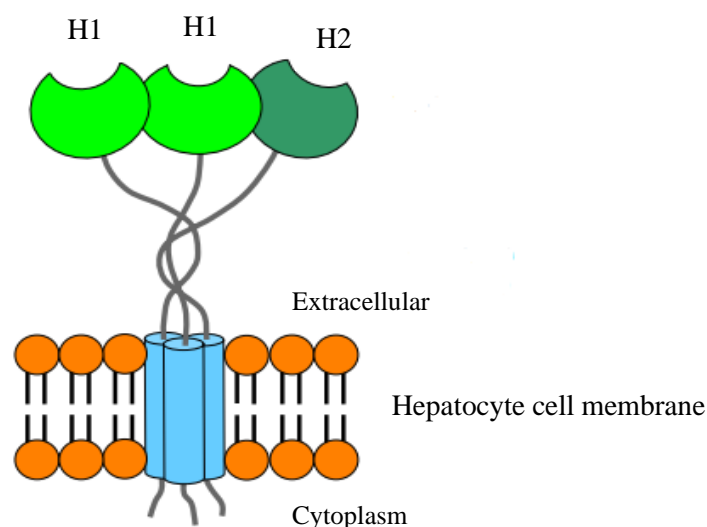


Figure 2. Schematical representation of ASGP receptor, with H1 and H2 subunits (adapted from Khorev *et al.*, 2018)

1.5. Nanotechnology and nanosystems

Stated the advances in the nanotechnology field, its application has been used in vast biomedical fields, such as drug carrier and drug delivery, gene therapy, molecular imaging, target therapy, biomarker mapping and detecting and diagnosis, thus nanomaterials possess high flexibility and versatility (Azevedo *et al.*, 2021; Chaturvedi *et al.*, 2018). There are numerous nanoscales materials, natural or synthetic, that can be used and combined such as nanoshells, gold nanoparticles, lipid nanoparticles, polymeric nanoparticles, micelles, cyclodextrins, carbon nanotubes, dendrimers and quantum dots (Figure 3) (Carthy *et al.*, 2014; Chaturvedi *et al.*, 2018). “Nanotechnology is the engineering and manufacturing of materials at the atomic and molecular scale” (Farokhzad *et al.*, 2009).

They possess unique physical and chemical characteristics such as nanoscale size, structure, chemistry and surface charge, that can be manipulated and changed to a certain purpose (Wicki *et al.*, 2015). The idea behind the different nanocarriers is to have a drug delivery system with the ability to encapsulate different therapeutic agents, such as drugs, genetic material and proteins, and promote a controlled and specific delivery of the same into the target cells. Therapeutic agents can be adsorbed, dissolved, encapsulated covalently attached or electrostatically bound to the nanoparticle (Azevedo *et al.*, 2021; Mc Carthy *et al.*, 2014). Thus, the use of nanomaterials might be of help in overcoming the limitations associated to conventional treatments and consequently increasing their efficacy and decreasing undesirable side-effects (Azevedo *et al.*, 2021; Bregoli *et al.*, 2016; Hossen *et al.*, 2019). Nanomaterials can facilitate

tissue penetration and improve delivery efficiency and specificity by carrying the therapeutic agents directly to the desired target. Furthermore, nanocarriers can encapsulate more than one therapeutic agent, allowing the development and application of combined strategies and the possible occurrence of a synergistic effect. Another important aspect of using nanomaterials is that they enable the encapsulation and transport of poorly soluble molecules and ensure the protection of the therapeutic agents, thus avoiding their degradation during transport/delivery, therefore improving their bioavailability (Azevedo *et al.*, 2021; Tran *et al.*, 2017; Wicki *et al.*, 2015; Wolfram and Ferrari., 2009).

Nanotechnology can also assist in molecular diagnosis of cancer, using nanoscale systems that can provide clear diagnostic clues of cancer, allowing an early detection of the malignancy (Bregoli *et al.*, 2016; Chaturvedi *et al.*, 2018). Given this, it is expected that development and further upgrade of nanotechnologies will play an important role in pharmaceutical industry and that their therapeutic applications will change the clinical landscape. Nanotechnology is used in the treatment of various diseases, including cancers. Cancer nanomedicine consists of using nanoparticles or nanomaterials for cancer-related biomedical purposes due to their unique characteristics and advantages (Azevedo *et al.*, 2021; Farokhzad *et al.*, 2009).

As many other drugs, the supra mentioned drugs, afatinib, BMS-777607 and XAV-939, do not possess specificity on the tumour targeting, and as a consequence these can induce negative side effects and healthy cells will also be affected, which would lead to undesired toxicity. Moreover, a high dose of drugs will be required in order to reach the cells, (Azevedo *et al.*, 2021; Zhang *et al.*, 2018). To solve these problems the drugs can be encapsulated in a hybrid nanosystem that delivers the drugs specifically to the hepatocellular carcinoma cells, avoiding its precocious release and spreading through the body, prolong their half-life in the systemic circulation, therefore increasing the efficacy of the drug delivery and decreasing its side effects. Multi drug resistance (MDR) has also been a problem in treating various types of cancer, due to the cells' capacity of developing molecular mechanisms to overcome the potential effect of the drugs, therefore, another important aspect to be retained is that nanosystems should have the ability to overcome the MDR (Azevedo *et al.*, 2021; Farinha *et al.*, 2021; Hossen *et al.*, 2018; Liu *et al.*, 2020; Yuan *et al.*, 2017; Zhang *et al.*, 2018).

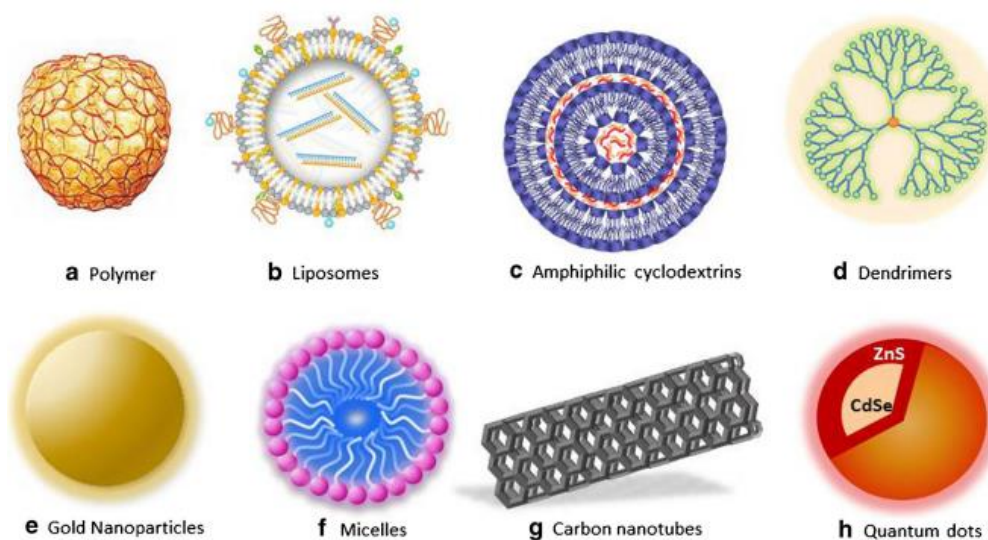


Figure 3. Different types of nanoparticles used for biomedical application (McCarthy *et al.*, 2014).

1.5.1. PLGA nanoparticles and liposomes

Polymeric nanoparticles have been largely used since they possess high structural integrity, stability during storage and a controlled release of the therapeutic agents. Polymeric nanoparticles can be produced out of natural polymers or synthetic polymers that are biocompatible and biodegradable, such as Poly(D,L-lactic-co-glycolic acid) (PLGA) polymer, which is a synthetic thermoplastic aliphatic biocompatible polyester. Previous studies reported that drugs that have been encapsulated in the PLGA nanoparticles had a controlled release, due to the fact that this polymer encapsulates the drug and forms a matrix (Gentile *et al.*, 2014; Nigam., *et al.*, 2019).

PLGA nanoparticles have the ability to encapsulate substances that possess different physico-chemical characteristics, such as proteins and drugs. PLGA is FDA approved biodegradable polymer that is commonly used as a carrier for drug delivery and as scaffolds for tissue engineering. It is biocompatible and has an excellent safety profile (Ding and Zhu., 2018). Usually, PLGA is produced by a catalysed ring-opening copolymerization of lactic acid (LA) and glycolic acid (GA) (Rezvantlab *et al.*, 2018). Therefore, PLGA chemical properties permit hydrolytic degradation through de-esterification that leads to metabolite monomers, lactic acid and glycolic acid. As the degradation occurs, the monomeric components of PLGA polymer are easily metabolized via the Krebs cycle, thus, are removed from the body by natural pathways (Danhier *et al.*, 2012; Gentile *et al.*, 2014).

Liposomes have also a great popularity as delivery systems, since they are considered ideal nanocarriers for drug delivery due to their high biocompatibility that is justified by the presence of phospholipids in their constitution (Hadinoto *et al.*, 2013). Natural phospholipids that are present in its formulation, are biodegradable, biocompatible, non-toxic and non-immunogenic. Liposomes have the ability to encapsulate different types of therapeutic molecules, such as drugs. Incorporation of compounds like cholesterol may assist with membrane fluidity and avoid premature drug leakage. Another important feature of liposomes is that they have the potential of increasing bioavailability and reduce clearance of drugs by increasing circulation and residence time in the body. In fact, they can prolong drugs half-life in the systemic circulation, and protect them from biodegradation *in vivo*, thus, allowing drugs to reach the target site in the desired concentration, avoiding the waste of the product and toxic effect in healthy tissues. (Fouladi *et al.*, 2017; Liu *et al.*, 2020; Shah *et al.*, 2020).

As to liposomes structure, these are self-assembled vesicles that have in their possession a phospholipid bilayer (it can be more than one). Its lipid composition confer stability to the liposomes and impact on their physicochemical and pharmacokinetic properties. Owing to the fact that phospholipids have an amphiphilic nature, liposomes can be a nanocarrier both to hydrophilic and lipophilic drugs. In this way, hydrophilic drugs are encapsulated in the aqueous core or attached to the membrane surface, in turn, hydrophobic drugs are incorporated into the lipid bilayer (Fouladi *et al.*, 2017; Liu *et al.*, 2020; Shah *et al.*, 2020).

Furthermore, liposomes loaded with the drug might accumulate in tumours via the enhanced permeability and retention (EPR) effect. In healthy tissues, the low-molecule-weight drugs might extravase the blood vessels, while drug-loaded liposomes won't, owing to their bigger size. Tumours blood vessels possess abnormally wide fenestrations that allow the extravasation of liposomes. Given this, along with the absence of lymphatic drainage, liposomes are selectively accumulated in tumours, becoming relatively more effective (Fouladi *et al.*, 2017; Li *et al.*, 2019)

1.5.2. Hybrid nanosystems

Hybrid nanosystems have been the centre of attention when it comes to biomedical biotech research projects, these can be obtained through the coordinated combination of materials, organic or inorganic, with different chemical composition (Figure 4) (Ferreira Soares *et al.*, 2020). Nanosystems can be used to transport and deliver different molecules, such as genetic material and drugs, through different stimuli (Date *et al.*, 2018; Hadinoto *et al.*, 2013; Torchilin., 2009). A combination between different organic and inorganic materials can be achieved to obtain a

polymer-hybrid nanoparticle (Ferreira Soares *et al.*, 2020; Peer *et al.*, 2007). The constituents to this purpose can be metal oxide nanoparticles, graphene, carbon nanotubes, silica and polymers. The combination between organic materials, such as phospholipids, proteins and lipids, with natural or synthetic polymers can give rise to hybrid-polymer nanosystems, in which hybrid-polymer nanosystems (LPNs) are included (Ferreira Soares *et al.*, 2020).

Among many others, lipids and polymers have been shown to be essential components to acquire LPN, due to their unique features and the most common ones are the polymer-core/lipid-shell systems. Polymer-core and lipid-shell nanosystems are constituted by a polymeric core in which therapeutic substances can be encapsulated. The polymeric core is coated by a lipidic layer, its main function is to confer biocompatibility and bioavailability to the nanosystem. It can also create a molecular fence that minimizes leakage of the encapsulated content in the polymeric core (Hadinoto *et al.*, 2013; Liu *et al.*, 2020). Therapeutic agents can also be encapsulated in the lipidic layer (Farinha *et al.*, 2021). By creating a LPN, the features, both of lipids and polymers are combined, overcoming some of the disadvantages, thus, a more integral, stable and multifunctional nanosystem can be obtained, with a more versatile usage (Liu *et al.*, 2020).

The combination of the different nanomaterials might result in advantages such as simultaneous transport of therapeutic agents with different properties, easier and longer nanosystem circulation in the blood stream, prevention from anticipated and non-specific release of the therapeutic agents, low encapsulation rate and unspecific release kinetics. Nanosystems can be used to transport and deliver different molecules, such as genetic material and drugs, through different stimuli (Hadinoto *et al.*, 2013; Ferreira Soares *et al.*, 2020; Wang *et al.*, 2019).

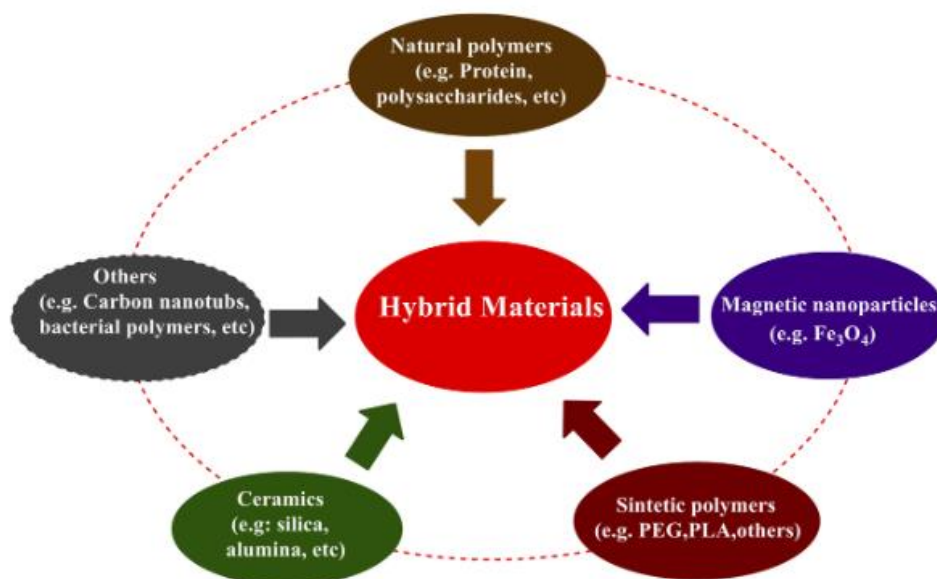


Figure 4. Different types of nanomaterials (organic or inorganic) used in the combination of hybrid nanosystems (Ferreira Soares *et al.*, 2020).

1.5.3. Nanosystem formulation for this project

In our laboratory a drug delivery hybrid nanosystem formulation was recently developed, being composed of a polymeric core and a lipidic shell containing the GalNAc ligand (Figure 5). The GalNAc ligand binds specifically to the ASGP receptors that are overexpressed in hepatocellular carcinoma cells (and almost absent in other tissues), making the nanosystem specific to the HCC cells, thus improving the therapeutic responses. In these hybrid nanosystems, drugs were encapsulated in the PLGA polymeric core and in the lipid bilayer (Farinha *et al.*, 2021).

The size of the nanosystems with the ligand GalNAc attached to the liposome, lightly increased, having a medium size of 150 nm (Figure 5B). Their zeta potential was positive before adding the GalNAc ligand and after its attaching it became negative, indicating that their physicochemical properties are suitable for *in vivo* application. An increased cellular internalization of the nanosystems prepared with the GalNAc ligand was observed, due to their specific binding to the ASGPR, demonstrating the specificity of the nanosystems to the HCC cells (Farinha *et al.*, 2021).

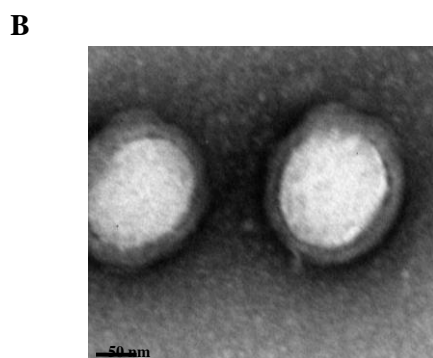
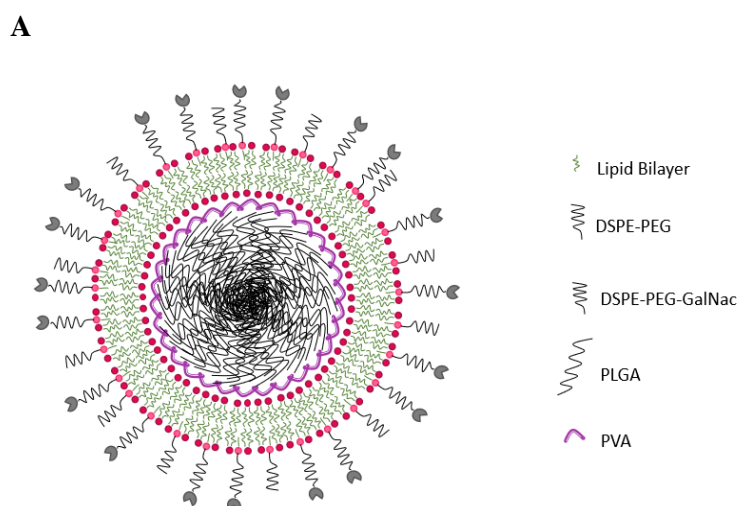


Figure 5. Representation of a hybrid nanosystem with polymeric core and lipidic shell (**A**) and its TEM image (**B**) (Farinha *et al.*, 2021).

1.6. Objective

Hepatocellular carcinoma is a highly malignant neoplasia, being the second cause of death in the world associated to cancer. Due to the absence of symptoms and effective screening strategies, advanced HCC stages are often diagnosed in patients with this disease. The available treatment to HCC is quite limited and with low rates of efficacy, therefore, the development of new and more effective antitumor approaches for HCC treatment is urgent.

Nanotechnology is widely used in the treatment of several diseases including cancers. Nanosystems possess unique characteristics with many advantages. These have the capacity of encapsulating different therapeutic agents and deliver them in the desired target. Moreover, nanosystems can provide protection to the encapsulated molecules, avoiding its leakage and degradation. Additionally, a specific delivery of the therapeutic agents into the target cells can be achieved through the nanosystems, resulting in a higher efficacy of the treatment and decreasing undesirable side-effects.

Afatinib, BMS-777607 and XAV-939 drugs are able to inhibit some of the major molecular targets that are overexpressed in hepatocellular carcinoma cells, such as EGFR, c-MET and WNT/ β -catenin, respectively. Lipid- and polymer-based nanosystems are versatile and stable nanocarriers capable of encapsulating drugs and delivering them safely and directly to the target. In this way, the main objective of this dissertation was to develop a new combined therapeutic strategy, involving afatinib, BMS-777607 and XAV-939 drugs, mediated by hybrid nanosystems, in order to obtain a synergistic antitumor effect against hepatocellular carcinoma cells.

The synergistic effect of the drugs, afatinib, BMS-777607 and XAV-939, was evaluated, that is, if the different combinations of the drugs are able to induce higher percentage levels of cytotoxicity to the HCC cells when compared to the sum of the cytotoxicity percentages of individual drugs applied in the same concentrations. Apoptosis/Necrosis assays were performed in order to understand the cellular death mechanisms occurring in the cells when treated with the drugs and drugs' combinations. Afterwards drugs were encapsulated in the hybrid nanosystems, PLGA nanoparticles and liposomes and the cell viability percentages of the HCC cells and their therapeutical potential was evaluated when incubated with these different formulations.

2. Materials and Methods

2. Materials and Methods

2.1. Materials

Poly(d,l-lactic-co-glycolic acid) (PLGA) 50:50 DL (24– 38kDa), polyvinyl alcohol (PVA) (MW 9000–10,000, 80% hydrolyzed), ethyl acetate (Sigma Aldrich), acetone, coumarin-6, Annexin V and propidium iodide were purchased from Sigma-Aldrich; 1-palmitoyl-2-oleoyl-sn-glycero-3-phosphocholine (POPC), cholesterol (Chol) and 1,2-distearoyl-sn-glycero-3-phosphoethanolamine-N-[amino(polyethylene glycol)-2000] (DSPE-PEG2000) were purchased from Avanti PolarLipids, Afatinib, BMS-777607 and XAV-939 were purchased from Selleckchem, triantennary N-acetylgalactosamine (GalNAc) cluster was kindly offered by Ionis Pharmaceuticals, asialofetuin (Sigma Aldrich) and didecyldimethylammonium bromide (DMAB) (Sigma Aldrich).

2.2. Methods

2.2.1. Hybrid nanosystem production and drug encapsulation

In the experimental section, we produced the hybrid nanosystems, that consist of a two-step method (Figure 6). Lipidic vesicles and PLGA nanoparticles are produced and the mixture of both is followed, giving rise to the lipid-polymer hybrid nanosystems. During the nanosystem production we proceeded to the drug (Afatinib, BMS-777607 and XAV-939) and coumarin-6 probe encapsulation in it. The encapsulation can occur in the core or the shell of the nanosystem. After that, we followed up to the drug quantification to verify the quantity of the drug that can be encapsulated in the nanosystem. A physical characterization of the nanosystems was repeated, its size and zeta potential were measured.

Drug quantification was performed through absorbance using a Spectofotometer Spectramax plus 384. First, the absorbance of each drug in dimethyl sulfoxide (DMSO) was determined through an absorbance spectre. Afatinib is 370nm, BMS-777607 is 340nm and XAV-939 is 350nm. After the nanoparticle production and drug encapsulation (with an initial amount of 1 mg of each drug), drug quantification was performed. To achieve this task, nanoparticles were freeze dried and briefly DMSO was added to the freeze-dried nanoparticles to disrupt them, in order to free the drug and read its absorbance. A standard curve of each drug was performed and the absorbance of the drug curve and drugs in the nanoparticle was read.

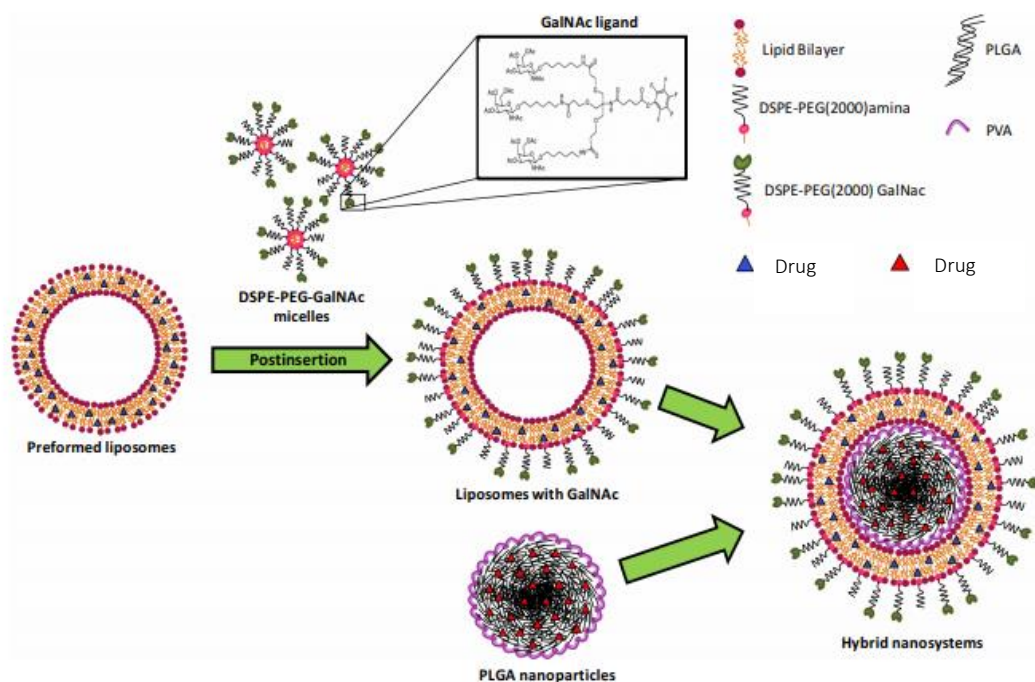


Figure 6. Schematic representation of the hybrid lipid-polymer nanosystem preparation with GalNAc ligand and drug encapsulation in the polymeric core or the lipidic shell (adapted from Farinha *et al.*, 2021).

2.2.1.1. PLGA nanoparticle production

First PLGA nanoparticles were produced by solvent emulsification and diffusion-evaporation method. PLGA 3% in ethyl acetate was poured in aqueous phase containing PVA 5%. This solution was stirred for 1 minute, using a sonication probe, with a 50% amplitude of sonication, in order to obtain an emulsion. When the drugs or coumarin-6 probe were encapsulated in the core of the nanoparticles, PLGA 3% in ethyl acetate and 20 μ l of each drug or 20 μ l of coumarin-6 (1 mg of drug/1 ml ethyl acetate and 1mg of coumarin-6/1 ml ethyl acetate) mixture was first stirred (300 rpm) for 30 minutes in room temperature and subsequently poured in aqueous phase containing PVA 5% and stirred (following the same steps described above). The resulting emulsion was diluted with water at 50 °C and stirred overnight to evaporate the organic solvent, ethyl acetate. In the next day the nanoparticles were centrifuged at 170000g and 25 °C for 25 minutes and resuspended with water (Figure 7).

Coated asialofetuin PLGA nanoparticles with PVA 5% and DMAB 2% surfactant were also produced, and the production method and drug and coumarin-6 encapsulation were similar to the described above. In this case DMAB surfactant was added to the mixture alongside with PLGA and PVA surfactant, a homogenizer (T 10 basic, Ultra Turrax, IKA) (20000 rotations/minute) was used, in order to obtain an emulsion, for 30 minutes (5 minutes stirring and

5 minutes in rest until reaching 30 minutes). Asialofetuin was added after the nanoparticle production (and drug or coumarin-6 encapsulation). In order to achieve a load complexation between the DMAB, with positive charge, and ASF, with a negative charge, we waited at least 20 minutes before using the nanoparticles.

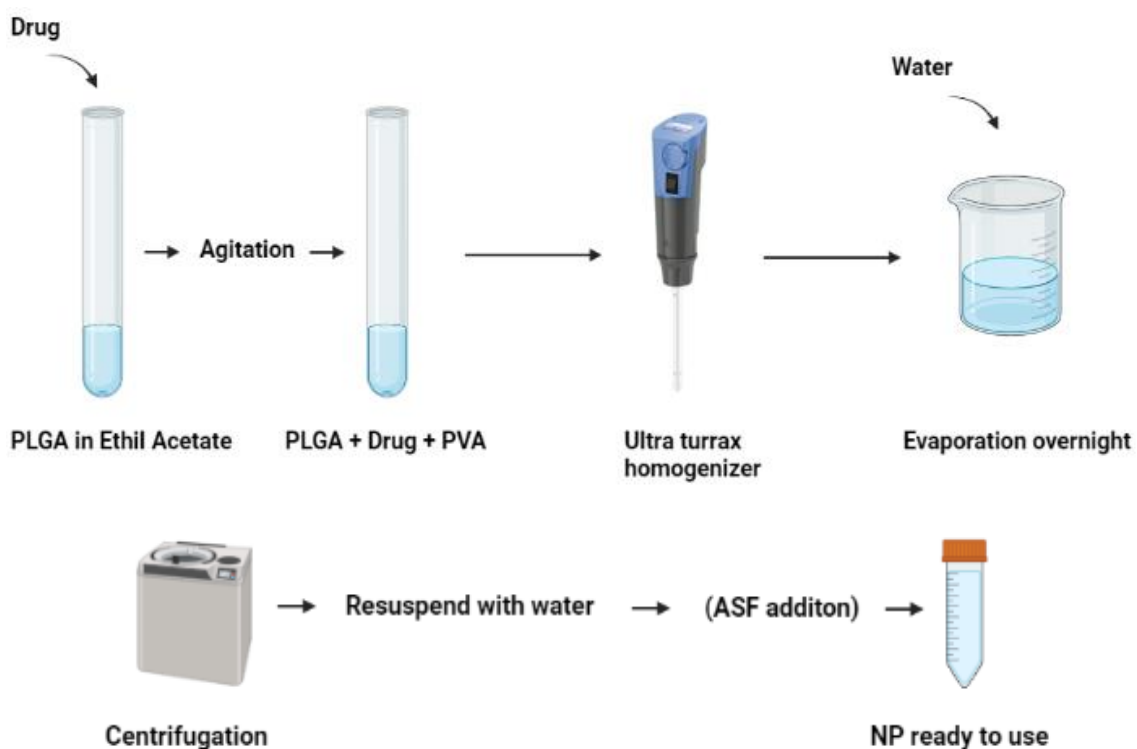


Figure 7. Schematic representation of the PLGA nanoparticle production.

2.2.1.2. Liposome production

Large unilamellar liposomes were prepared by extrusion of multilamellar liposomes composed of 1:1 (molar ratio) mixtures of 1-palmitoyl-2-oleoyl-sn-glycero-3-phosphocholine (POPC) and cholesterol. POPC, cholesterol, DSPE-PEG2000 lipids were dissolved in chloroform and dried with nitrogen. Posteriorly, the originating lipidic film was hydrated with deionized water and sonicated for 5 min (Figure 8). Liposomes that were produced with the GalNAc ligand underwent a postinsertion method. The method of DSPE-PEG2000-GalNAc production consisted with the GalNAc PFP ester dissolved in acetone was coupled to DESPE-PEG2000-amine micelles that were prepared in sodium tetraborate buffer at pH 8.5. To obtain a couple reaction of these two components these were stirred overnight. Afterwards, GalNAc O-acetyl groups were removed by the addition of aqueous ammonia and micelles were purified by size exclusion

chromatography using water as running buffer to remove unreacted GalNAc. The insertion of DESPE-PEG-GalNAc conjugates or DESPE-PEG-amine onto the liposomes was performed (at 2% ml relative to the total lipid amount) through micelles incubation with liposomes in a water bath at 40 °C for 16 hours under agitation. The drugs and coumarin-6 probe were encapsulated in the lipidic bilayer during the process of the liposomes production. 0.2mg of each drug in 5.34 mg of lipids (with a 30µg of drug/mg of liposome loading capacity), and 40µl of coumarin (1mg/ml of chloroform) in 2.67 mg of lipid (15µl of coumarin-6/mg of liposome of loading capacity).

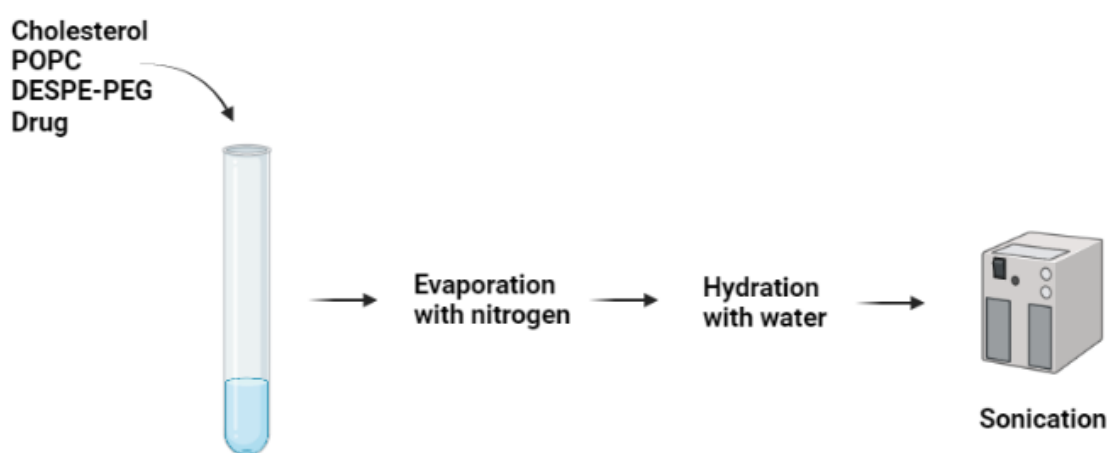


Figure 8. Schematic representation of the liposome production.

2.2.1.3. Hybrid nanosystems production

Hybrid nanosystems were originated by the addition of the PLGA nanoparticles to the performed liposomes (Figure 6) containing the DESPE-PEG-GalNAc or DESPE-PEG-amine, with a 4/1 PLGA/lipid ratio. The mixture of both was vortexed for 1 hour at 50 °C and 300 rpm.

2.2.2. Characterization of nanoparticles

After the production of PLGA nanoparticles and addition of ASF in case of ASF-coated PLGA nanoparticles, the nanoparticles were diluted in water and its size were measured.

Characterization of the nanoparticles was performed in order to come across of its average hydrodynamic diameter, polydispersity index and zeta potential. As to the dynamic light scattering (DLS) measurements of the nanoparticles these were performed using a Zetasizer Nano-ZS (Malvern Instruments Ltd., UK). With the assistance of the software Zetasizer 7.02 nanoparticles measurements were converted into average hydrodynamic diameter and polydispersity index. Characterization of the nanoparticle's zeta potential was also performed using Zetasizer Nano-ZS (Malvern Instruments Ltd., UK), which is able to measure electrophoretic and zeta mobility potential distribution using a method of light scattering by phase analysis. These tests were performed under 25°C, in water, and a backward scattering angle of 173°.

2.2.3. Cell culture

Hepatocellular carcinoma cells, HepG2, Hep3B and Huh7 were kept in culture in Dulbecco's modified Eagle's medium (DMEM) under 37° and 5% CO₂. The culture medium consists of 10% (v/v) heat-inactivated fetal bovine serum (FBS), penicillin (100 U/ml) and streptomycin (100 U/ml). The HepG2, Huh7 and Hep3B cells were seeded at a density of 60×10^3 cells/cm², 60×10^3 cells/cm² and 30×10^3 cells/cm² respectively.

2.2.4. Cell viability

Different combinations of free drugs and nanosystems loaded drugs were tested. These combinations were administered to the hepatocellular carcinoma cell lines, HepG2, Hep3B and Huh7. Drug concentrations were defined according to the IC₅₀ of each drug. Subsequently, we proceeded to the evaluation of the drug combination and chose the better ones, the ones with higher efficiency of HCC cells cytotoxicity and better synergistic effect. For this purpose, viability tests, Alamar Blue viability assays were performed.

To verify the levels of cytotoxicity of the free drugs (Afatinib, BMS-777607 and XAV-939), nanosystems/nanoparticles or liposome loaded with drugs on the HCC cells, Alamar Blue assays were performed. In this assay it is possible to measure the redox capacity of the cells, due to the production of metabolites that results from the cell growth. Resazurin is an active ingredient of the Alamar Blue reagent, as it enters the living cells, resazurin is reduced to resorufin, which emits high red fluorescence. Cells were seeded in 96-well culture plates and after 24h these were incubated with different conditions of drugs for 72h. After 72h of incubation the medium was

vacuumed. Alamar blue dye 10% (v/v) that was previously prepared (from a 0.1 mg/mL stock solution of alamar blue), was added to the cells and left for 1h under 37 °C and 5% CO₂. Subsequently, the absorbance was read, using a SPECTRAMax PLUS 384 spectrophotometer at 570 and 600 nm length after, approximately, 1h of incubation at 37 °C. Cell viability was calculated using the formula: $(A_{570} - A_{600})$ of treated cells $\times 100 / (A_{570} - A_{600})$ of control cells.

2.2.5. Cellular uptake and Internalization of the nanoparticles

HepG2 cells were seeded in the 12-well culture plates, after 24h each well was incubated with previously prepared nanoparticles (with ASF or not) and liposomes loaded with a fluorescent probe, coumarin-6. Coumarin-6 is a dye that can be used to label and visualise nanoparticles. It has an excitation peak at 457 nm and an emission peak at 501 nm. A 4-hour incubation at 37 °C was followed and subsequently the cells were washed with PBS, detached and resuspended with trypsin. Afterwards, the cell medium was added and the cells were homogenised. Briefly, the cells were transferred to cytometry tubes and centrifuged at 950rpm for 5 minutes at 4 °C. The supernatant was removed. PBS was added and another centrifugation (with the same conditions) took place, this procedure must be repeated twice in order to remove all of the medium. Subsequently, the analysis of the samples was performed through flow cytometry (FACSCalibur flow cytometer, Becton Dickinson, NJ, USA) and data was analysed with the assistance of the CellQuest software.

2.2.6. Cellular death mechanisms

Cellular death of the hepatocellular carcinoma cells after the drug administration was established and it was evaluated whether cellular death occurs via apoptosis or necrosis. The combination of two probes, FITC-Annexin V and PI (propidium iodate) allow us to verify the way that the cellular death proceeds. The cells were seeded at the 24-well culture plates and after 24h the cells were incubated with the free drugs combinations. After a 72h incubation, cell media and cells that were washed with PBS and detached with trypsin were harvested and transferred to the cytometry tubes. Posteriorly, the cells were centrifuged at 300g for 5 minutes at 4 °C. The supernatant was removed and the cells were resuspended in 1ml of binding buffer (10mM HEPES (pH 7.4), 2.5mM CaCl₂, 140mM NaCl) and centrifuged once more. The supernatant was removed and cells were resuspended in 100µl of binding buffer containing 2µl of FITC annexin V (0.05 mg/ml) and 1µl of PI (0.05 mg/ml). Samples were incubated for 15 minutes in the dark at room

temperature and centrifuged, 200µl of binding buffer was added and the cells were finally analysed in the FACSCalibur flow cytometer (Becton Dickinson NJ, USA). The fluorescence of FITC was evaluated in the FL-1 channel and PI fluorescence was evaluated in the FL-3 channel. Afterwards, the data was analysed using CellQuest software.

3. Results

3. Results

3.1. Incubation of HCC cell lines with different combinations of free drugs

Hepatocellular carcinoma cell lines, HepG2, Hep3B and Huh7, were treated with the different drug combinations and concentrations (1 μ M, 0.5 μ M and 0.25 μ M), below the IC₅₀ of the drugs, and after 72h of incubation cell viability was measured using Alamar Blue assay, in order to evaluate the antitumor potential of the different drug combinations, by comparing them with the cell viability levels obtained after cells incubation with the individual drugs.

3.1.1. Afatinib and XAV-939 combination in HepG2, Hep3B and Huh7 cells

The effect on the cell viability of the free drugs afatinib (AFT) and XAV-939 (XAV), both individually or in combination, was firstly evaluated in HepG2 cells (Figure 9A). The obtained results show that the lower concentrations of the individual drugs did not result in a significant cytotoxicity, only the concentration of 1 μ M of the isolated drugs promoted a significant reduction on the cell viability, approximately 44% of cytotoxicity. Regarding the drug combinations, when AFT and XAV were combined at the smaller concentrations only a slight decrease in the cell viability was observed, as compared to that registered after HepG2 cells treatment with the same amount of each individual drug. However, when the drugs were combined with, at least, one them at the highest tested concentration (AFT 0.25 μ M/XAV 1 μ M; AFT 0.5 μ M/XAV 1 μ M; AFT 1 μ M/XAV 0.25 μ M; AFT 1 μ M/XAV 0.5 μ M; and AFT 1 μ M/XAV 1 μ M), a strong reduction on cell viability levels (43.11%; 39.16%; 42.74%; 37.56%; 20.48%, respectively) was observed. The cytotoxicity induced by these combinations was slightly higher than the sum of the cytotoxicity obtained with the same amount of the isolated drugs, indicating that most of these drug combinations resulted in a small synergistic effect in HepG2 cells.

In Hep3B cells (Figure 9B), isolated AFT and XAV presented reduced cytotoxicity when their concentrations were low. A slight reduction on cell viability (approximately 60% and 78%) occurred when the concentrations reached 1 μ M. When AFT and XAV were combined, overall, there was no significant reduction in the cell viability. AFT 0.25 μ M/XAV 0.25 μ M, AFT 0.25 μ M/XAV 0.5 μ M, AFT 0.25 μ M/XAV 1 μ M, AFT 0.5 μ M/XAV 0.25 μ M, AFT 0.5 μ M/XAV 0.5 μ M and AFT 0.5 μ M/XAV 1 μ M combinations presented low synergistic effect for different cell viability percentages (82.33%, 84.03%, 65.19%, 78.71%, 74.08% and 54.33% respectively).

Combinations like AFT 1 μ M/XAV 0.25 μ M, AFT 1 μ M/XAV 0.5 μ M and AFT 1 μ M/XAV 1 μ M induced lower cell viability level, but no synergistic effect was detected, given that the sum of the levels of cell cytotoxicity of isolated drugs is higher than in these combinations.

As to Huh7 cell line (Figure 9C), a more proportional decrease on the cell viability occurred, given to the fact that a proportional decrease of cell viability levels was observed as the concentrations of each drug increase. Once more, lower percentages of individual drugs did not result in high levels of cytotoxicity and slightly increased with 1 μ M. As the drugs were combined a reduction in the cell viability was also proportional to the concentration of the drugs. Combinations of AFT 0.25 μ M/XAV 0.25 μ M, AFT 0.25 μ M/XAV 0.5 μ M, AFT 0.25 μ M/XAV 1 μ M, AFT 0.5 μ M/XAV 0.25 μ M, AFT 0.5 μ M/XAV 0.5 μ M, AFT 0.5 μ M/XAV 1 μ M, AFT 1 μ M/XAV 0.25 μ M, AFT 1 μ M/XAV 0.5 μ M and AFT 1 μ M/XAV 1 μ M yielded cell viability percentages of 97.18%, 79.02%, 39.00%, 67.87%, 56.90%, 24.57%, 42.32%, 30.29% and 10.88%, respectively. Combinations like AFT 0.25 μ M/XAV 1 μ M and AFT 0.5 μ M/XAV-939 1 μ M exhibited a significant synergistic effect, since these combinations presented a difference of cytotoxic of 18.75% and 17.87%, respectively, when compared with the sum of the cytotoxicity of isolated drugs in these concentrations.

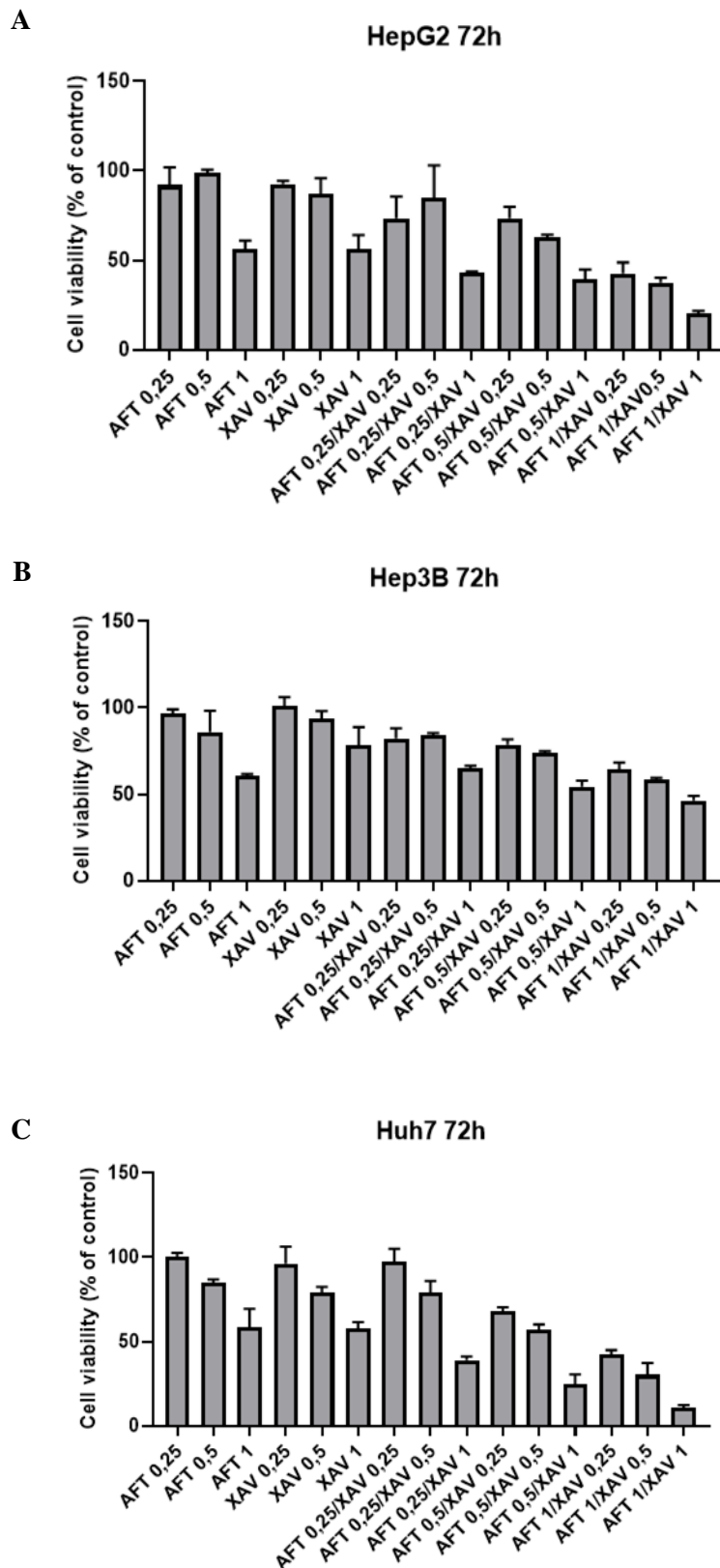


Figure 9. Therapeutic potential of the different combinations and concentrations of Afatinib (AFT) and XAV-939 (XAV) drugs. HepG2 (A), Hep3B (B) and Huh7 (C) cells were treated with different concentrations (0.25 μ M, 0.5 μ M and 1 μ M) and combinations of free drugs (with individual drugs as controls). The cells were incubated for 72h and subsequently viability of the same were analysed using the Alamar blue assay in the three independent assays.

3.1.2. BMS-777607 and Afatinib combination in HepG2, Hep3B and Huh7 cells

Another combination was made with afatinib and BMS-777607 (BMS) in the same concentrations as in previous study with AFT and XAV, 1 μ M, 0.5 μ M and 0.25 μ M. In HepG2 cells (Figure 10A), the same profile was observed as to isolated drugs, lower concentrations yielded higher cell viability levels and lower when the drugs' concentrations were higher. Positive results came when these two drugs were combined, all of the combinations possess synergy. Combination of BMS 0.25 μ M/AFT 0.25 μ M, BMS 0.25 μ M/AFT 0.5 μ M, BMS 0.25 μ M/AFT 1 μ M, BMS 0.5 μ M/AFT 0.25 μ M, BMS 0.5 μ M/AFT 0.5 μ M, BMS 0.5 μ M/AFT 1 μ M, BMS 1 μ M/AFT 0.25 μ M, BMS 1 μ M/AFT 0.5 μ M and BMS 1 μ M/AFT 1 μ M resulted in cell viability percentages of 77.76%, 79.17%, 42.80%, 72.36%, 52.06%, 38.42%, 54.19%, 36.69% and 6.06%, respectively. Most of the conditions had an approximate 20% difference in cytotoxicity between the combinations and the sum of cytotoxicity of the corresponding isolated drugs. The combination BMS 0.5 μ M/AFT 0.5 μ M resulted in a difference of 45,87% in cell viability, when compared to the corresponding isolated drugs.

In Hep3B cells (Figure 10B), most of the combinations presented synergistic effect, which are BMS 0.25 μ M/AFT 0.25 μ M, BMS 0.25 μ M/AFT 1 μ M, BMS 0.5 μ M/AFT 0.25 μ M, BMS 0.5 μ M/AFT 1 μ M, BMS 1 μ M/AFT 0.25 μ M and BMS 1 μ M/AFT 1 μ M with BMS 0.25 μ M/AFT 0.5 μ M, BMS 0.5 μ M/AFT 0.5 μ M and BMS 1 μ M/AFT 0.5 μ M as the exceptions. The best combinations were BMS 0.5 μ M/AFT 1 μ M and BMS 1 μ M /AFT 1 μ M that resulted in 39.55% and 9.59% of cell viability, respectively.

Comparing to HepG2 and Hep3B cells, Huh7 (Figure 10C) was the cell line that exhibited less combinations with synergistic effect. Only four of the tested combinations presented synergistic effect, these were BMS 0.25 μ M/AFT 1 μ M, BMS 0.5 μ M/AFT 0.5 μ M, BMS 0.5 μ M/AFT 1 μ M and BMS 1 μ M/AFT 1 μ M that resulted in 45.43%, 57.13%, 29.48% and 5.47% of cell viability, respectively. Although these percentages are low, there was no such evident synergistic effect when compared to the cytotoxicity induced by isolated drugs. The most effective synergy was obtained with the BMS 0.25 μ M/AFT 1 μ M combination, in which the registered cytotoxicity was 54.57% and the difference of cytotoxicity between the combination and the sum of cytotoxicity for isolated drugs in these concentrations was 28.55%. BMS 1 μ M/AFT 1 μ M condition presented a very high toxicity, but the difference between the induced cytotoxicity of the combination and the isolated drugs was only 13.47%.

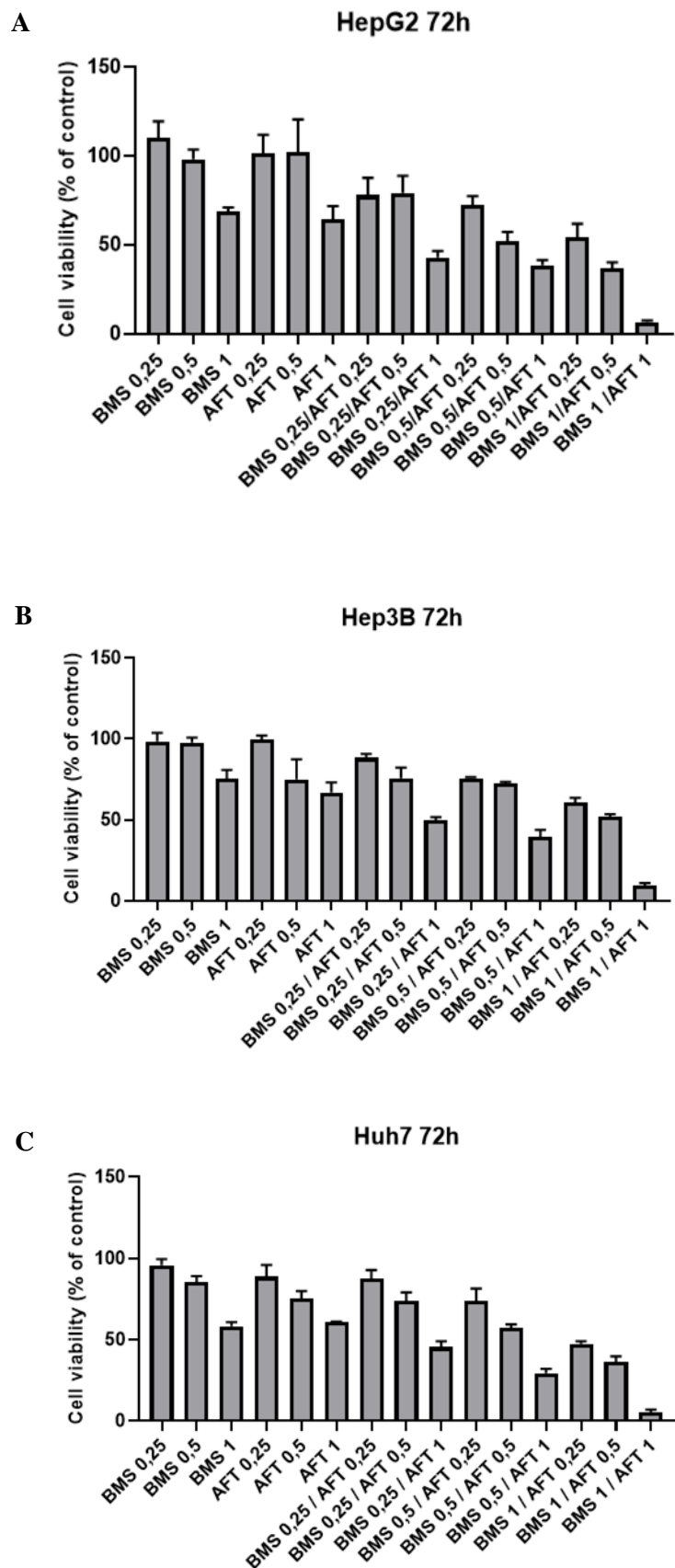


Figure 10. Therapeutic potential of the different combinations and concentrations of BMS-777607 (BMS) and Afatinib (AFT) drugs. HepG2 (A), Hep3B (B) and Huh7 (C) cells were treated with different concentrations (0.25 μ M, 0.5 μ M and 1 μ M) and combinations of free drugs (with individual drugs as controls). The cells were incubated for 72h and subsequently viability of the same were analysed using the Alamar blue assay in the three independent assays.

3.1.3. BMS-777607 and XAV-939 combination in HepG2, Hep3B and Huh7 cells

Further on, combination between BMS-777607 (BMS) and XAV-939 (XAV) was evaluated the same way previous combinations were, following the same profile of combinations and concentrations. All the cell lines, HepG2, Hep3B and Huh7, presented high cell viability levels when treated with low concentrations of isolated drugs, and slightly lower with higher concentrations. Similarly, to what happened in afatinib and BMS-777607 combination, in HepG2 cell line the combination between BMS and XAV (Figure 11A) resulted in synergy in all of the combinations, and in some cases, pretty notable ones. The two best combination in this assay were BMS 1 μ M/XAV 0.5 μ M and BMS 1 μ M/XAV 1 μ M, since these resulted in very low cell viability levels 34.59% and 3.83%, respectively. Moreover, the synergy observed in these combinations was very effective. The difference between the percentages of cytotoxicity of the combinations and isolated drugs was 29.74% and 26.77%, thus these conditions increase the cellular death by ~30% compared to isolated drugs. Another great synergistic effect was obtained with BMS 0.5 μ M/XAV 0.5 μ M combination. Although the cell viability associated to this combination was 60%, it possesses a notable synergy, since toxicity of this condition compared to the sum of isolated drugs was 30.84% higher.

In Hep3B cell line (Figure 11B) only in two combinations synergistic effect did not occur, but the synergy existing in the other combinations was not as outstanding as in HepG2 line. Conditions with relatively notable synergy were BMS 0.25 μ M/XAV 1 μ M, BMS 0.5 μ M/XAV 0.25 μ M and BMS 0.5 μ M/XAV 1 μ M in which the difference of these combinations and the sum of percentage of toxicity of isolated drugs were 15.48%, 11.79% and 13.25%, respectively. Conditions that did not possess synergy were BMS 0.5 μ M/XAV 0.5 μ M and BMS 1 μ M/XAV 0.25 μ M.

In Huh7 cells (Figure 11C), likewise in HepG2, all of the conditions hold synergy. The condition that resulted in a better synergistic effect was BMS 0.5 μ M/XAV 1 μ M, the cellular death induced by this combination was high, 69.94%, and it was 20.48% higher than that obtained with the sum of the isolated drugs. The combinations BMS 0.25 μ M/XAV 1 μ M, BMS 0.5 μ M/XAV 0.5 μ M and BMS 1 μ M/XAV 1 μ M were the next ones in line regarding their synergistic potential. The latter combination, BMS 1 μ M/XAV 1 μ M, resulted in a high cytotoxicity, 87.77%, but its synergy is not as striking.

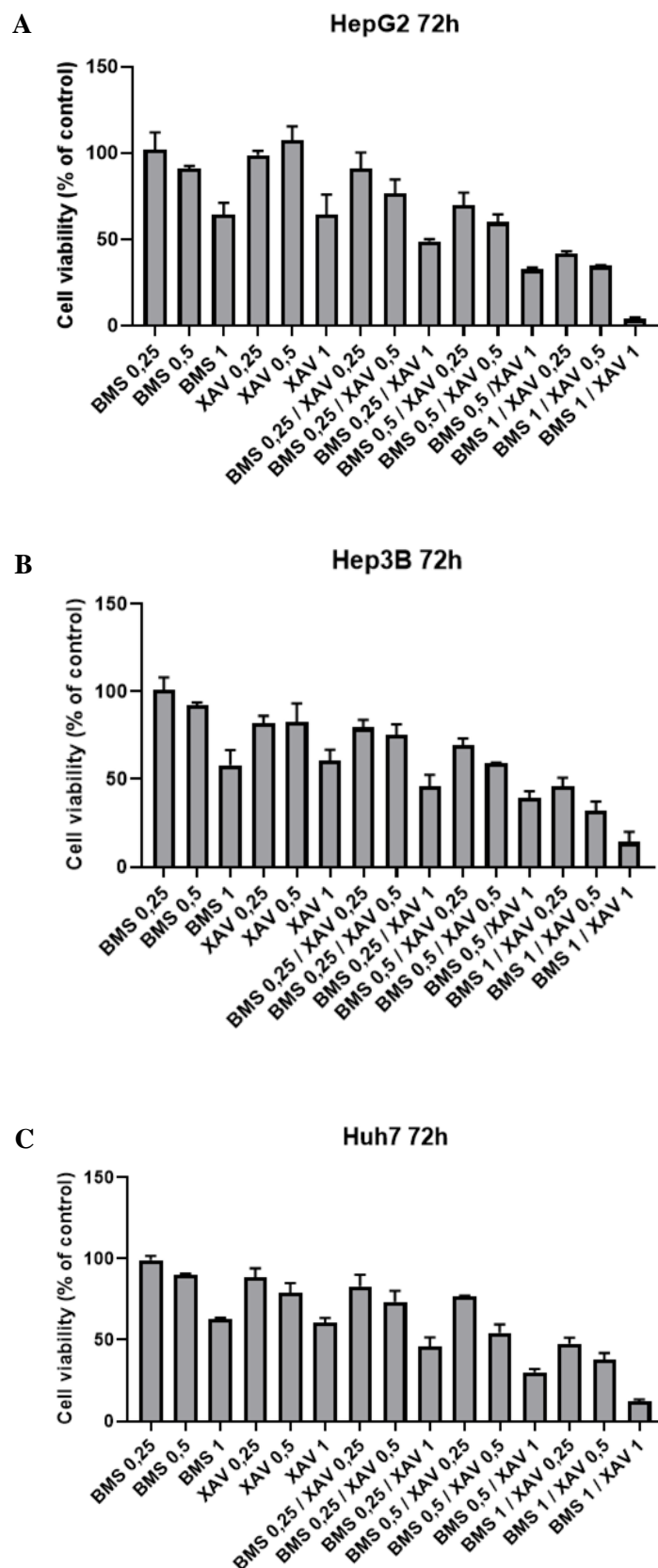


Figure 11. Therapeutic potential of the different combinations and concentrations of BMS-777607 (BMS) and XAV-939 (XAV) drugs. HepG2 (A), Hep3B (B) and Huh7 (C) cells were treated with different concentrations (0.25 μ M, 0.5 μ M and 1 μ M) and combinations of free drugs (with individual drugs as controls). The cells were incubated for 72h and subsequently viability of the same were analysed using the Alamar blue assay in the three independent assays.

3.1.4. BMS-777607, afatinib and XAV-939 combination in HepG2 and Hep3B

Given the positive results regarding drug combination in pairs, combinations with the three drugs were tested in HepG2 and Hep3B cells. Concentrations of the drugs were chosen accordingly to the results achieved with previous combinations, in order to obtain new combinations of three drugs that work positively together and reach a more outstanding synergy. In HepG2 cell line (Figure 12A), some of the combinations of the three drugs resulted in a remarkable synergy. Surely, some combinations were better than others in this matter.

According to the obtained results in HepG2 cells with isolated drugs, it was observed high cell viability when the drugs were used at 0.25 μ M and 0.5 μ M, followed by a decrease when the concentration was 1 μ M. Different combinations were tested, the ones with a striking synergistic effect were: BMS 0.5 μ M/AFT 0.5 μ M/XAV 0.5 μ M, BMS 0.5 μ M/AFT 0.5 μ M/XAV 0.25 μ M, BMS 1 μ M/AFT 0.25 μ M/XAV 0.25 μ M, BMS 1 μ M/AFT 0.5 μ M/XAV 0.25 μ M; BMS 0.25 μ M/AFT 1 μ M/XAV 0.5 μ M, BMS 0.25 μ M/AFT 1 μ M/XAV 0.25 μ M and BMS 0.5 μ M/AFT 0.5 μ M/XAV 1 μ M, since these combinations induced high cellular death, 72.62%, 56.08%, 46.19%, 58, 08%, 62.27%, 50.69% and 48.62%, respectively, when compared to that registered with the sum of the cytotoxicity promoted by the equivalent isolated drugs.

In Hep3B cell line (Figure 12B), after incubation with 1 μ M afatinib, an unusual drop to 30.52% in cell viability occurred, even though all the combination conditions, except two, presented a synergistic effect. The best combinations were: BMS 0.5 μ M/AFT 0.5 μ M/XAV 0.5 μ M, BMS 0.5 μ M/AFT 0.25 μ M/XAV 0.25 μ M, BMS 0.5 μ M/AFT 0.5 μ M/XAV 0.25 μ M, BMS 1 μ M/AFT 0.5 μ M/XAV 0.25 μ M and BMS 0.5 μ M/AFT 0.5 μ M/XAV 1 μ M. These combinations resulted in low cell viability percentages, 24.70%, 46.07%, 34.89%, 12.69% and 7.50%, respectively.

After the analysis of the results of the cellular viability, it is possible to infer that some of the conditions, in which the drugs are combined, either in pairs or the three altogether, show a strong synergistic effect and that their antitumor potential could be effective to hepatocellular carcinoma treatment.

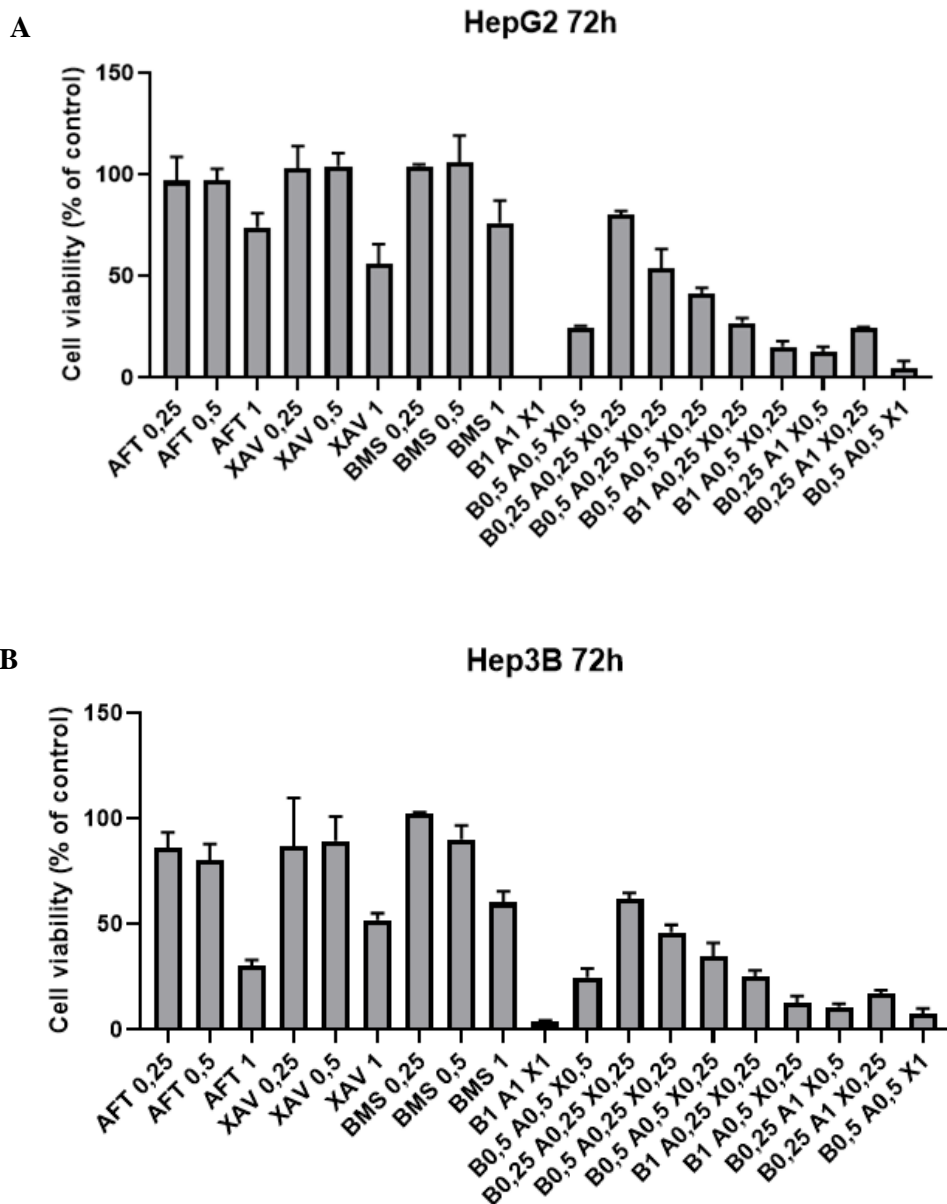


Figure 12. Therapeutic potential of the different combinations and concentrations of Afatinib (AFT), BMS-777607 (BMS) and XAV-939 (XAV) drugs. HepG2 (A) and Hep3B (B) cells were treated with different concentrations (0.25µM, 0.5µM and 1µM) and combinations of free drugs (with individual drugs as controls). The cells were incubated for 72h and subsequently viability of the same were analysed using the Alamar blue assay in the three independent assays.

3.2. Apoptosis/necrosis of HCC cells treated with the combination of free drugs

The cellular membrane is composed of a lipid bilayer, and phosphatidylserine (PS) in one of the lipids that can be found in the inner leaflet of the plasma membrane, and consequently it is only exposed to the cell cytoplasm. During early apoptosis PS is exposed on the outer leaflet of the plasma membrane, and the fluorescent probe Annexin V binds to it emitting fluorescence. This way, Annexin V can be used to detect early apoptotic cells. On the other hand, Annexin V can also stain necrotic or late apoptotic cells, since during necrosis and late apoptosis the cell membrane ruptures exposing PS, Annexin V can have access to the entire plasma membrane, as well as PI. Propidium iodide is unable to enter early apoptotic cells as these haven't reached the phase of the membrane integrity loss. As soon as the cellular membrane disintegrates, which happens during late apoptosis and necrosis, PI is now able to enter the cells. Subsequently it binds to the DNA of the cells and emits fluorescence.

After verifying the efficacy of the free drugs to induce cytotoxicity to HCC cells, PI and Annexin V were used in order to determine if cellular death occurs through apoptosis and/or necrosis. To this study, we chose some of the most promising drug combinations presented above (BMS 1 μ M/ AFT 1 μ M; BMS 1 μ M/ XAV 1 μ M; BMS 0.5 μ M/ AFT 0.5 μ M/ XAV 0.5 μ M; BMS 1 μ M/ AFT 0.25 μ M/ XAV 0.25 μ M; BMS 0.25 μ M/ AFT 1 μ M/ XAV 0.5 μ M), and incubated HepG2 cells with them for 72h, before performing Annexin V and PI staining. The obtained results, show that these drug combinations induce cellular death mostly through apoptosis (Figure 13, 14 and 15). Our control condition, consisting of untreated HepG2 cells (Figure 13), presented 83.46% of living cells, 11.98% of cells in early apoptosis and 3.04% of cells in late apoptosis/necrosis. The conditions corresponding to treatment with individual drugs (Table 1 and Figure 14A) have a similar profile to the control cells, being the living cells the predominant ones, followed by cells undergoing early apoptosis and a lesser percentage of cells in late apoptosis and/or necrosis. When cells were incubated with the combinations of the drugs (Table 2 and Figure 14B) the scenario changed, the percentage of living cells decreased, and the percentages of early apoptotic cells and cells in late apoptosis and/or necrosis rose. All combinations, except for BMS 1 μ M/AFT 1 μ M, were associated to early apoptosis as the leading cellular death mechanism, nevertheless percentages of cells in late apoptosis or necrosis were also present. The combination in which early apoptosis corresponded to the higher percentages was BMS 0.25 μ M/AFT 1 μ M/XAV 0.5 μ M. In this condition the percentage of living cells was 1.065%, the percentage of cells in early apoptosis was 65.13% and in late apoptosis and/or necrosis was 33.78%. BMS 1 μ M/XAV 1 μ M and BMS 0.5 μ M/AFT 0.5 μ M/ XAV 0.5 μ M were also conditions

that yielded high percentages of apoptosis with 50.26% and 52.84% respectively (all of the values represented are mean values).

Table 1. Percentages of living, apoptotic and necrotic HepG2 cells after 72h of incubation with different drug concentrations.

Condition	Living cells	Early apoptotic cells	Late apoptotic or necrotic cells
BMS-777607 0.25μM	89.97%	6.68%	2.59%
BMS-777607 0.5μM	81.72%	14.95%	2.98%
BMS-777607 1μM	72.14%	16.81%	9.04%
Afatinib 0.25μM	87.97%	10.03%	1.82%
Afatinib 0.5μM	79.81%	16.96%	2.94%
Afatinib 1μM	59.17%	34.37%	6.39%
XAV-939 0.25μM	85.01%	9.90%	3.40%
XAV-939 0.5μM	79.75%	14.23%	5.00%
XAV-939 1μM	72.01%	22.36%	5.12%

Table 2. Percentages of living, apoptotic and necrotic HepG2 cells after 72h of incubation with different drug combinations and concentrations.

Condition	Living cells	Early apoptotic cells	Late apoptotic or necrotic cells
BMS 1μM/AFT 1μM	3.93%	45.62%	50.03%
BMS 1μM/XAV 1μM	2.93%	50.26%	46.49%
BMS 0.5μM/AFT 0.5μM/XAV 0.5μM	24.22%	52.84%	22.71%
BMS 1μM/AFT 0.25μM/XAV 0.25μM	45.78%	39.09%	14.48%
BMS 0.25μM/AFT 1μM/XAV 0.5μM	1.06%	65.13%	33.78%

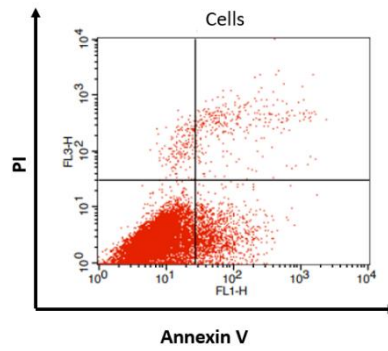


Figure 13. Apoptosis levels in untreated HepG2 cells after 72h of being plated. Annexin V and PI were used to detect cell in early apoptosis and late apoptosis/necrosis. The apoptosis levels of cells were analysed by flow cytometry. Two independent assays were performed.

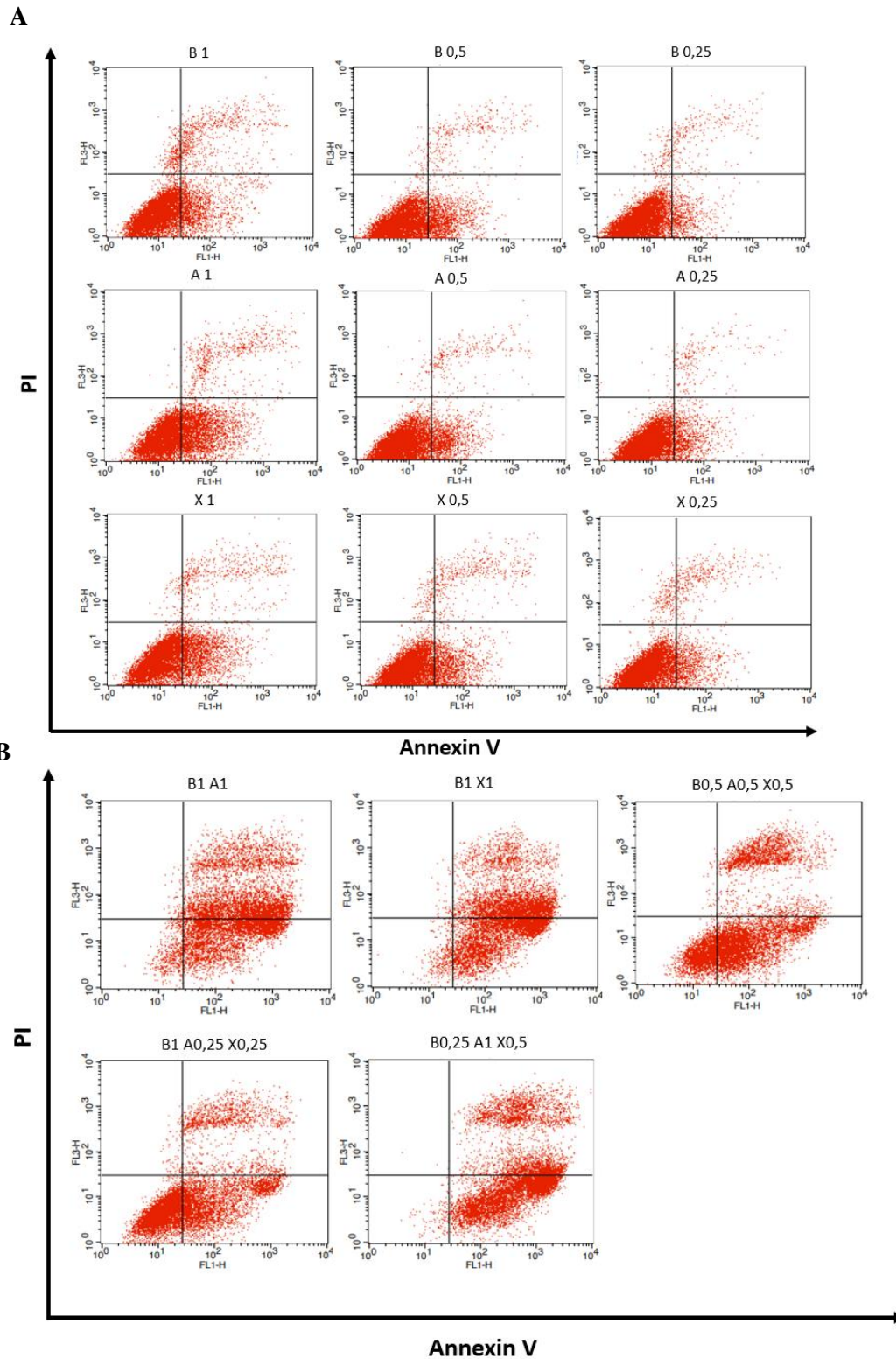


Figure 14. Apoptosis levels promoted by free drugs (Aftatinib (AFT), BMS-777607 (BMS) and XAV-939 (XAV)) **(A)** and drugs combinations (BMS 1 μ M/ AFT 1 μ M; BMS 1 μ M/ XAV 1 μ M; BMS 0.5 μ M/ AFT 0.5 μ M/ XAV 0.5 μ M; BMS 1 μ M/ AFT 0.25 μ M/ XAV 0.25 μ M; BMS 0.25 μ M/ AFT 1 μ M/ XAV 0.5 μ M) **(B)** in different concentrations (0.25 μ M, 0.5 μ M and 1 μ M) in HepG2 cells that were stained with Annexin V and PI double-staining for 15 min after being treated, for 72 hours, with the drugs and drugs combinations. The apoptosis levels of cells were analysed by flow cytometry. Two independent assays were performed.

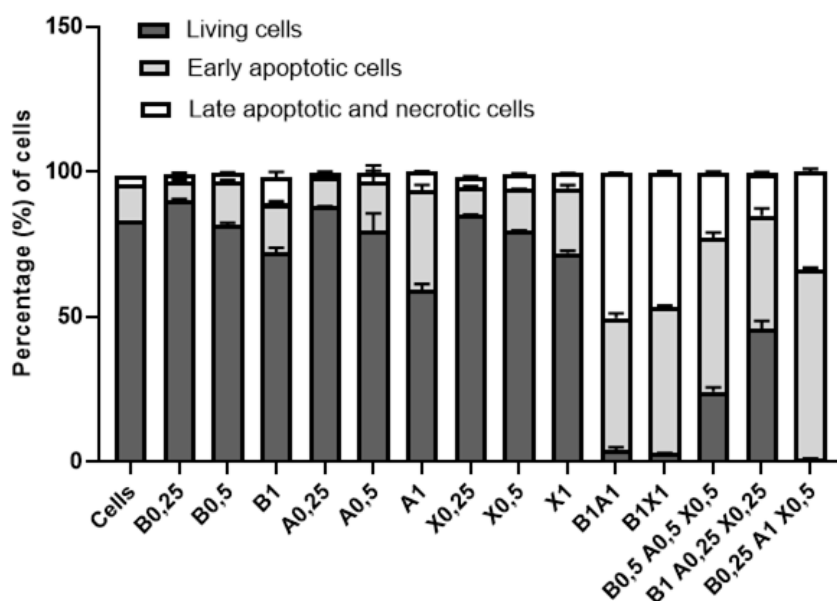


Figure 15. Graphical representation of living cells and apoptosis/necrosis percentages promoted by different drug concentrations (0.25 μ M, 0.5 μ M and 1 μ M) of isolated drugs and different drug combinations (BMS 1 μ M/ AFT 1 μ M; BMS 1 μ M/ XAV 1 μ M; BMS 0.5 μ M/ AFT 0.5 μ M/ XAV 0.5 μ M; BMS 1 μ M/ AFT 0.25 μ M/ XAV 0.25 μ M; BMS 0.25 μ M/ AFT 1 μ M/ XAV 0.5 μ M) in HepG2 cells after 72h of incubation. The percentages of live cells, cells in early apoptosis and cells in late apoptosis/necrosis were presented in bar graphs. Annexin V and propidium iodide probes were used to detect early apoptotic cells and late apoptotic/necrotic cells. The apoptosis levels of cells were analysed by flow cytometry. Two independent assays were performed.

3.3. Production of hybrid nanosystems

3.3.1. Optimization of the PLGA nanoparticles using a sonication probe

Production of PLGA nanoparticles was optimized using a sonication probe. Different strategies were tested to obtain the best nanoparticle formulation, the one capable of encapsulating a good amount of drugs and presenting suitable physicochemical properties. Time and amplitude of the sonication were tested as well as the PLGA percentage. After the nanoparticles size measurement, it was determined that the preparation conditions used to encapsulate the drugs would be: 1 minute of sonication, with a 50% of amplitude, and PLGA 3 % (Table 3).

The first formulation was prepared with three minutes of sonication, 60% sonication amplitude and PLGA at 2 %. The size of the resulting nanoparticles was $99,3 \pm 0,48$ nm. In the subsequent preparation the amplitude of the sonication was increased to 90 % and the time was

decreased from three minutes to one minute, resulting in an increase of the nanoparticles size to 110.7 ± 1.42 nm. As this size was not a favourable one according to our goal, we kept altering and testing sonication time and the percentage of sonication amplitude. The condition in which sonication time was one minute and the amplitude was 50 % resulted in 113.8 ± 0.49 nm nanoparticle size. To obtain a slightly bigger nanoparticle formulation, PLGA percentage was altered from 2% to 3%, and the obtained size was 118.6 ± 0.36 nm, with a low polydispersity index (0.060 ± 0.012). This formulation was the chosen one to encapsulate the drugs. There seems to be a small tendency in the nanoparticles size increase when the sonication time is decreased. The same goes to sonication amplitude, as the amplitude is reduced, nanoparticles size increases. However, statistically, these results don't seem to be significant. More notable differences were observed when PLGA percentage was increased, when the percentage of PLGA was increased from two to three percent, nanoparticles size was bigger.

Table 3. Influence of the different PLGA nanoparticle preparation conditions in their size (mean(nm)) and Polydisperse index (P.I.).

Nanoparticle	Mean (nm)	P.I.
3 min / 60% amp PLGA 2%	99.3 ± 0.48	0.108 ± 0.030
1 min / 90% amp PLGA 2%	110.7 ± 1.42	0.046 ± 0.018
1 min / 70% amp PLGA 2%	109.7 ± 2.03	0.081 ± 0.033
1 min / 50% amp PLGA 2%	113.8 ± 0.49	0.038 ± 0.026
1 min / 50% amp PLGA 3%	118.6 ± 0.36	0.060 ± 0.012

3.3.2. Production of hybrid nanoparticles, encapsulation of the drugs and evaluation of their therapeutic potential

Given the positive results regarding drug combinations in terms of therapeutic potential, we proceeded to the encapsulation of the 3 drugs, Afatinib (AFT), BMS-777607 (BMS) and XAV-939 (XAV), in the PLGA nanoparticles (Table 4). We started off with 1 mg of each drug and after that proceeded with its quantification.

As the drugs were encapsulated in PLGA nanoparticles, the ones encapsulating AFT and XAV maintained its size 116 ± 2.05 nm and 117 ± 4.89 nm. Nanoparticles encapsulating BMS increased their size to 125.1 ± 3.63 nm. Polydisperse index is under 0.2 thus the resulted

nanoparticles were not polydisperse (Table 4). Afterwards, as the encapsulation of the drugs in the nanoparticles was achieved, quantification assays of the drugs were accomplished to determine the loading efficiency and loading capacity of each drug in the nanoparticles (Table 5). AFT and XAV had a low loading efficiency, 7.9% and 7.7% respectively. The loading capacity also presented low values, 3.9 μg of drug/mg of NP and 2.3 μg of drug/mg of NP for AFT and XAV, respectively. In contrast, BMS presented a high loading efficiency, 67.9%, and 19.53 μg of drug/mg of NP of loading capacity.

Table 4. Size and Polydisperse index of drug-loaded PLGA nanoparticles.

Nanoparticle/Drug	Mean (nm)	P.I.
Empty	118.6 \pm 0.36	0.060 \pm 0.012
Afatinib	116.5 \pm 2.05	0.093 \pm 0.026
BMS-777607	125.1 \pm 3.63	0.148 \pm 0.030
XAV-939	117 \pm 4.89	0.069 \pm 0.056

Table 5. Loading capacity e loading efficiency of the PLGA nanoparticles.

Drug	Loading capacity (μg of drug/mg of NP)	Loading efficiency (% of encapsulated drug)
Afatinib	3.9	7.9%
XAV-939	2.3	7.7%
BMS-777607	19.53	67.9%

Considering that the loading efficiencies of AFT and XAV in PLGA nanoparticles were low, these drugs were encapsulated in the liposomes, in order to improve those levels. Therefore, we proceeded with the encapsulation of 0.2 mg of each drug in 5.34 mg of lipids, which means that the loading capacity is of 37.4 μg /mg of liposome.

As PLGA nanoparticles encapsulating BMS and liposomes encapsulating AFT and XAV were produced, we carried on to the hybrid nanosystems preparation and obtained four different hybrid nanosystems (Empty NP + empty liposomes (NPV); Empty NP + AFT liposomes (A);

Empty NP + XAV liposomes (X); BMS NP + empty liposomes (B)). Subsequently, hepatocellular carcinoma cells were incubated with the resulted hybrid nanosystem. Two different drug combinations, that were already tested with free drugs (BMS 0.5 μ M/AFT 0.5 μ M/XAV 0.5 μ M and BMS 1 μ M/AFT 0.25 μ M/XAV 0.25 μ M), were also tested in hybrid nanosystems. Then, cell viability was evaluated after incubation with the different hybrid nanosystems encapsulating the drugs (Figure 16 and 17).

First, the BMS 0.5 μ M/AFT 0.5 μ M/XAV 0.5 μ M condition was tested in HCC cells lines. HepG2, Hep3B and Huh7 cells were incubated with the produced hybrid nanosystems and the obtained cell viability results are illustrated in Figure 16. According to the results, in HepG2 cell line (Figure 16A), it was observed that this condition (represented by BAX) resulted in a 27.18% of cytotoxicity. Free drugs induced higher cytotoxicity, the viability of the cells registered in the presence of free drugs was 21.85%. In Hep3B (Figure 16B) and Huh7 (Figure 16C) cells, the cytotoxicity induced by the drug combination, mediated by the hybrid nanosystems, was lower in comparison to that obtained in HepG2 cell line, being not significant. In these cell lines, the free drugs combination promoted cell viability levels of 25 %.

The drug combination consisting of BMS 1 μ M/AFT 0.25 μ M/XAV 0.25 μ M, mediated by the hybrid nanosystems followed the high cell viability level profile for HepG2 and Huh7 cell line (Figure 17). Contrary to the first condition, in which HepG2 cells showed lesser cell viability, in this case, Hep3B (Figure 17B) was the cell line that presented the lower levels of cell viability, 63.56%. HepG2 and Huh7 cell lines presented similar levels of cell viability (Figure 17A and 17C), with 92.41% for HepG2 cells and 92.42% for Huh7. The free drugs combination promoted low cell viability levels, 23.51%, 13.27% and 24.22% to HepG2, Hep3B and Huh7, respectively.

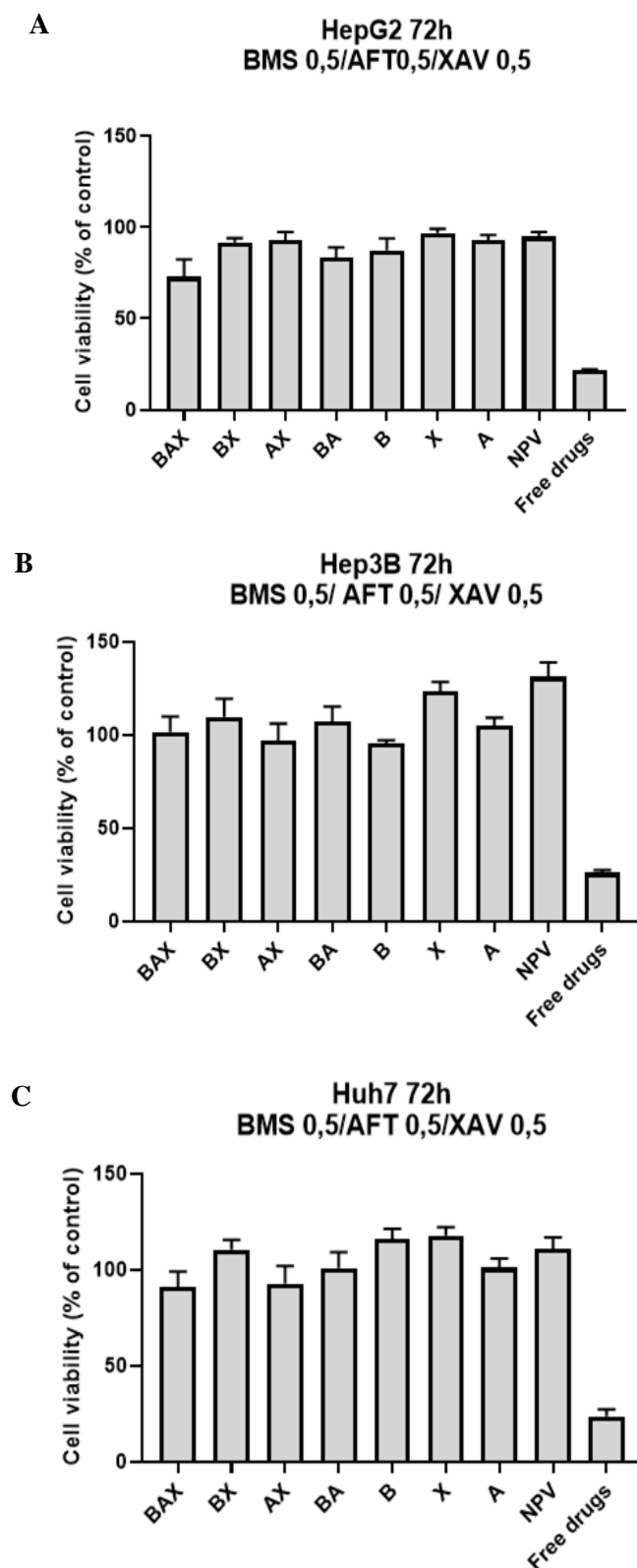


Figure 16. Therapeutic potential of the different hybrid nanosystems encapsulating Afatinib, BMS-777607 and XAV-939 drugs and free drugs in BMS 0.5 μ M/ AFT 0.5 μ M/ XAV 0.5 μ M combination. HepG2 (**A**), Hep3B (**B**) and Huh7 (**C**) cells were treated with hybrid nanosystems and free drugs. The cells were incubated for 72h and subsequently cell viability were analysed using the Alamar blue assay in three independent assays. **NPV** is for empty NP + empty liposome, **B** is for BMS-777607 NP + empty liposome, **A** is for empty NP + Afatinib liposome, and **X** is for empty NP + XAV liposome.

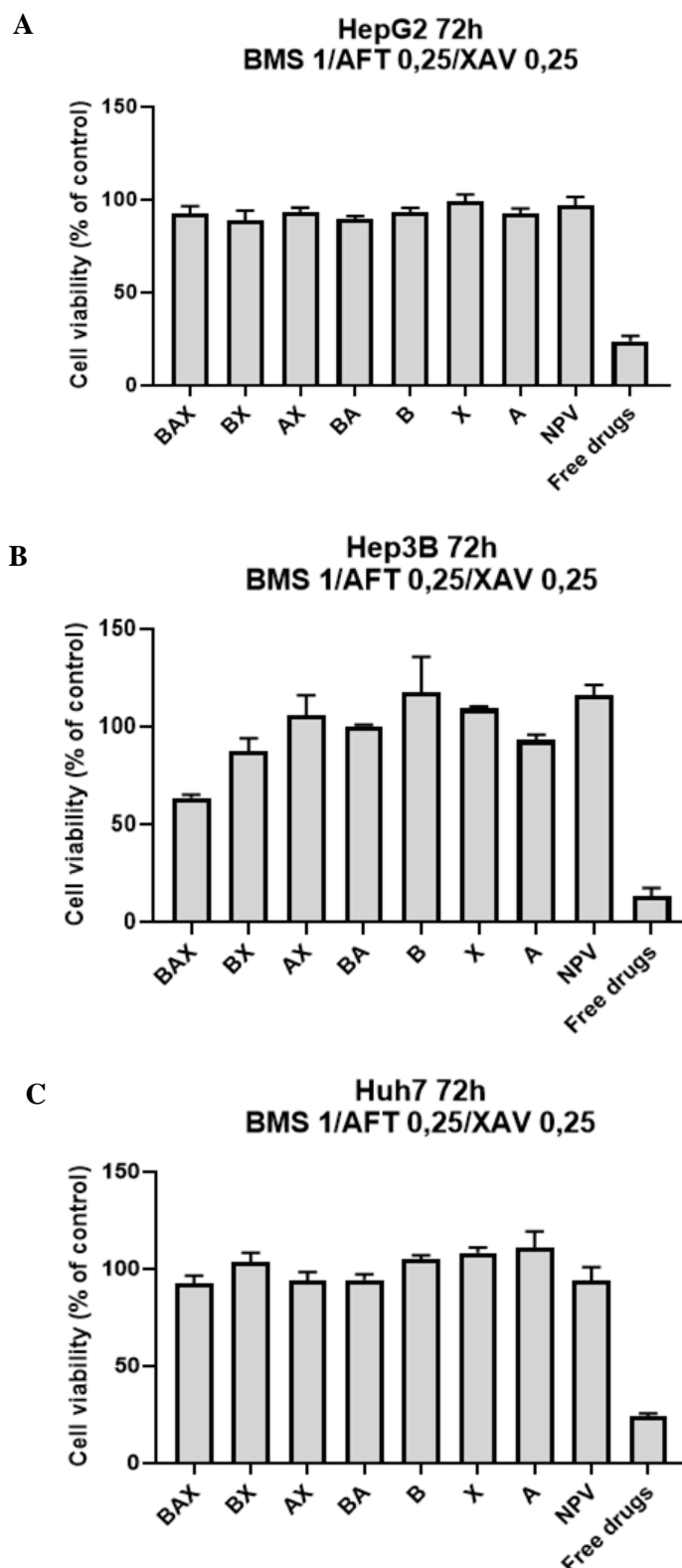


Figure 17. Therapeutic potential of the different hybrid nanosystems encapsulating Afatinib, BMS-777607 and XAV-939 drugs and free drugs in BMS 1 μ M/ AFT 0.25 μ M/ XAV 0.25 μ M combination. HepG2 (A), Hep3B (B) and Huh7 (C) cells were treated with hybrid nanosystems and free drugs. The cells were incubated for 72h and subsequently cell viability were analysed using the Alamar blue assay in three independent assays. NPV is for empty NP + empty liposome, B is for BMS-777607 NP + empty liposome, A is for empty NP + Afatinib liposome and X is for empty NP + XAV liposome.

3.4. Production of Asialofetuin-coated PLGA nanoparticles loaded with BMS-777607 and evaluation of their therapeutic potential

Considering the previous results regarding hybrid nanosystems and given the fact that only BMS-777607 drug had a good encapsulation in the PLGA nanoparticles, we prepared isolated PLGA nanoparticles encapsulating BMS-777607, 1 mg of the drug. Ultra turrax homogenizer was used to stir the mixture. Afterwards, Asialofetuin (ASF), which is a ligand of the ASGPR that is overexpressed in the HCC cells, was added in different concentrations to the nanoparticles in order to coat them, since the positive charge of the DMAB, at the nanoparticles surface, allows the establishment of electrostatic interactions with the negative charge of the ASF. Subsequently, an extra wash of the particles was performed in order to remove the excess of DMAB to prevent toxicity of the same to the cells by bursting their lipidic bilayer.

First, we tested different concentrations of ASF to cover the nanoparticle surface (0/25/50/75/100/125/150 μg ASF/mg NP), in order to identify the ASF concentration that could allow the high level of cellular binding and internalization of the PLGA nanoparticles (Figure 18). Flow cytometry assays were performed with nanoparticles loaded with a fluorescent probe, coumarin-6, to determine the internalization of the nanoparticles with different ASF concentration in HepG2 cells. Overall, all of the nanoparticles prepared with the different ASF concentrations were internalized by the cells, independently of the ASF concentration. Nevertheless, the formulation consisting of 125 μg ASF/mg NP was chosen to mediate the drug delivery process since it presented a slightly higher level of cellular internalization (94.50 of Geo Mean) (Figure 18 and 19).

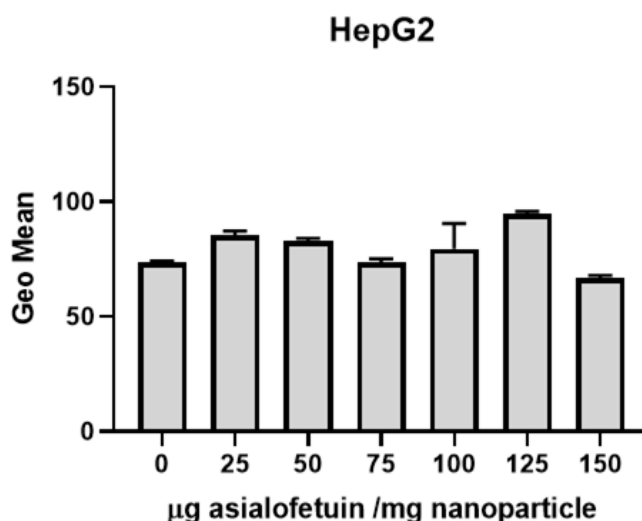


Figure 18. Effect of different asialofetuin concentrations on the cellular internalization of PLGA nanoparticles in HepG2 cells evaluated by flow cytometry. Coumarin-6 probe was previously encapsulated in the nanoparticles in order to perform this assay. ASF concentration was of 0, 25, 50, 75, 100, 125, 150 μg ASF/mg NP

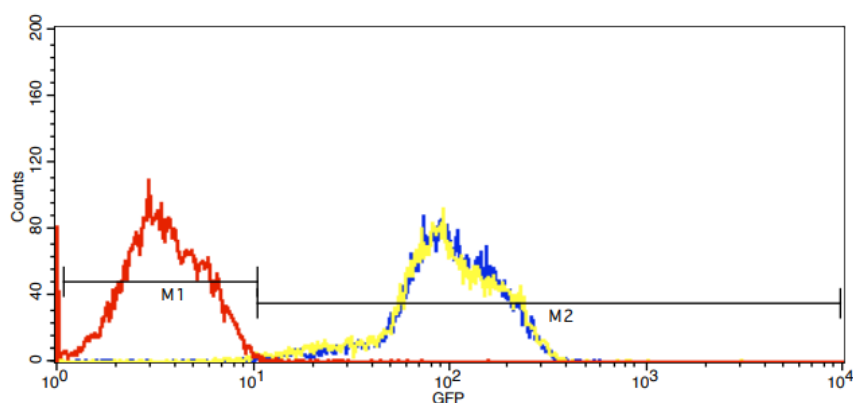


Figure 19. Effect of asialofetuin concentration on the cellular internalization of PLGA nanoparticles in HepG2 cells evaluated by flow cytometry. M1 is for untreated cells and M2 is for cellular internalization of PLGA nanoparticles with 125 μg ASF/mg NP. Coumarin-6 probe was previously encapsulated in the nanoparticles in order to perform this assay. Red represents untreated cells, blue and yellow represent PLGA nanoparticles with 125 μg ASF/mg NP in duplicate.

In the absence of ASF (0 μg ASF/mg NP) an internalization of the nanoparticles in the cells occurred through an unspecific binding, given that the cells' surface is negatively charged and the zeta potential of these nanoparticles was positive, giving rise to electrostatic interactions. Nevertheless, when ASF concentration was 125 μg ASF/mg NP, even though zeta potential of these nanoparticles was negative, a high internalization of these nanoparticles still occurred (Figure 20).

Nanoparticles without ASF presented a positive zeta potential, 19.9 mV. However, when ASF, that possesses negative charge, was added to the nanoparticles, the zeta potential of the formulation 125 μg ASF/mg NP become negative, -9.02 mV (Table 6). The size of the nanoparticles slightly increased, from 94.78 nm to 113.4 nm, when ASF (125 μg ASF/mg NP) was present in the nanoparticles (Table 6).

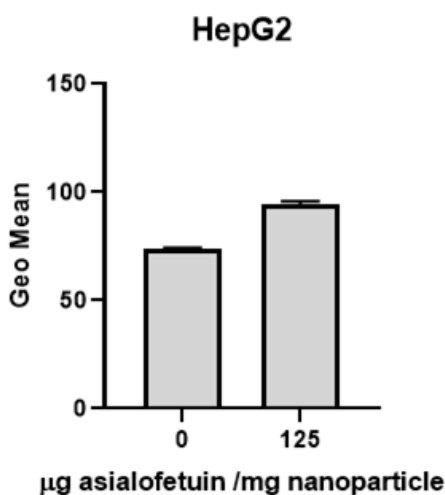


Figure 20. Effect of asialofetuin association to PLGA nanoparticles (0/125 μg ASF/mg NP) on their cellular internalization in HepG2 cells evaluated by flow cytometry. Coumarin-6 probe was previously encapsulated in the nanoparticles in order to perform this assay.

Table 6. Physicochemical characterization of the PLGA Nanoparticle.

Asialofetuin concentration (μg ASF/mg NP)	Zeta potential (mV)	Size (nm)
0	19.9	94.78
125	-9.02	113.5

Thereafter we proceeded with the cell viability assays, after the 72h of cells incubation with empty nanoparticles and nanoparticles encapsulating BMS-777607 (Figure 21). Both, the empty and drug-loaded nanoparticles, were tested in different concentrations, 2.5 μg , 5 μg , 7.5 μg

and 10 μ g of nanoparticle/well. The drug concentration in the wells, for each nanoparticle condition, is presented in the Table 7.

Table 7. Drug mass for each nanoparticles condition.

PLGA nanoparticle	BMS-777607
2.5 μ g	0.096 μ g
5 μ g	0.192 μ g
7.5 μ g	0.289 μ g
10 μ g	0.384 μ g

The obtained results (Figure 21) show that there was an increase in the cytotoxicity to the HepG2 cells when the nanosystems were loaded with BMS-777607, compared to the empty ones. According to the obtained data, the conditions that stood out were B 7.5 NP/0 ASF, B 10 NP/0 ASF, B 7.5 NP/125 ASF and B 10 NP/125 ASF (that resulted in very low cell viability levels, 7.40%, 3.58%, 12.75% and 7.69%, respectively, showing the ability of the PLGA nanoparticles to deliver the BMS into the HCC cells. However, there were no notable differences between the nanoparticles prepared with or without asialofetuin. In addition, the empty nanoparticles resulted by themselves in a significant toxicity, that increased with the nanoparticles concentrations, although being always much lower than that observed with drug-loaded nanoparticles.

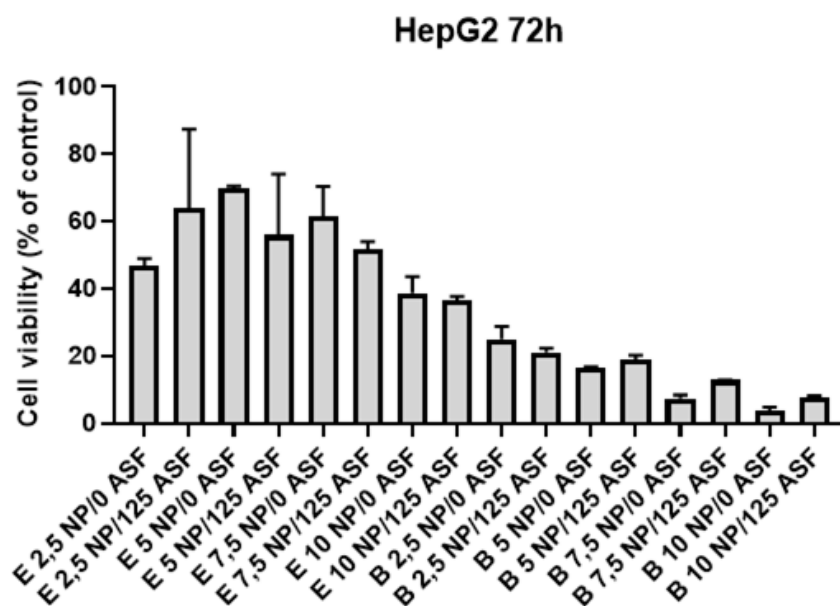


Figure 21. Graphical representation of the therapeutic potential of the different combinations of PLGA nanoparticles, empty and loaded with BMS-777607 drug. HepG2 cells were treated with different concentrations (2.5 μ g, 5 μ g, 7.5 μ g or 10 μ g) of empty nanoparticles and nanoparticles loading BMS-777607 drug. Asialofetuin was attached to the nanoparticles in two different concentrations (0 or 125 μ g ASF/mg NP). The cells were incubated for 72h and subsequently viability of the same were analysed using the Alamar blue assay. In the figure, **NP** is for nanoparticles and **ASF** is for asialofetuin. **E** means that the nanoparticles are empty. **B** means that the nanoparticles are loaded with BMS-777607 drug. **2.5, 5, 7.5** or **10 NP** refers to the nanoparticle's concentrations, that can be 2.5 μ g, 5 μ g, 7.5 μ g or 10 μ g. **0** or **125 ASF** refers to the concentration of the asialofetuin present in the nanoparticles, that can be 0 or 125 μ g ASF/mg NP.

3.5. Production of liposomes loaded with afatinib, BMS-777607 and XAV-939 drugs and evaluation of their therapeutic potential

In order to take advantage of the synergistic antitumor effect observed with the drug combination involving AFT, BMS and XAV, these drugs were encapsulated in the liposomes. Before moving forward, we made sure that liposomes were internalized by HCC cells. Flow cytometry assays were performed with liposomes (loaded with coumarin-6) in different concentrations (10 μ g, 25 μ g, 50 μ g, 100 μ g and 200 μ g). The obtained results show that the cellular internalization of the liposomes efficiently occurred, being proportional to the liposomes concentration, the higher the concentration the higher the internalization by the cells (Figure 22). When the liposome amount was 200 μ g, the Geo Mean value for the internalization was 244.89, when the amount dropped to 50 μ g, so did the internalization to 155.88.

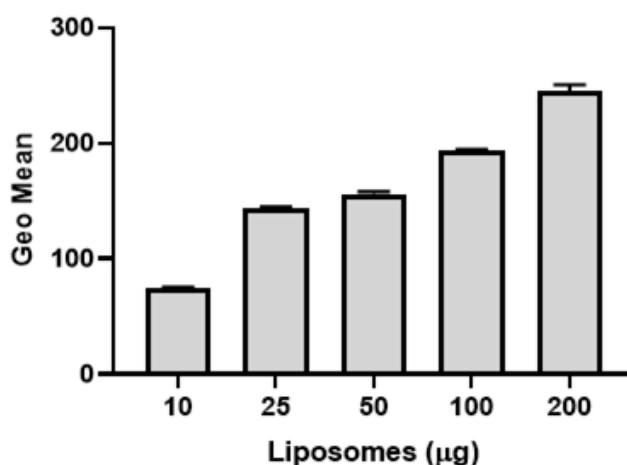


Figure 22. Effect of different liposome concentrations on the cellular internalization in HepG2 cells evaluated by flow cytometry. Liposome concentrations were of 10, 25, 50, 100 and 200 μ g. Coumarin-6 probe was previously encapsulated in the liposomes in order to perform this assay.

Afterwards, we proceeded with the liposome production and process of encapsulation of the drugs, 0.2 mg of each drug in 5.34 mg of lipids. Four different liposomes were obtained (Empty liposomes (NPV), afatinib liposomes (A), BMS-777607 liposomes (B) and XAV-939 liposomes (X)). The same conditions of the drug combinations, BMS 0.5 μ M/AFT 0.5 μ M/XAV 0.5 μ M and BMS 1 μ M/AFT 0.25 μ M/XAV 0.25 μ M, that were tested with free drugs and the hybrid nanosystems, were tested with the liposomes as well.

The first condition to be tested was BMS 0.5 μ M/AFT 0.5 μ M/XAV 0.5 μ M. HepG2 and Hep3B cells were incubated for 72h with the liposomes encapsulating the drugs and then cell viability was evaluated (Figure 23). In HepG2 cells (Figure 23A), this condition (represented by BAX) resulted in high values of cell viability, 89.91 %, while free drug combination promoted a decrease of cell viability to 31.64 %. In Hep3B cells (Figure 23B), this condition yielded an increase in the cytotoxicity, reducing the cell viability to 75.89%, that is even more significant when compared to the cell viability registered with empty liposomes, 122.60 %.

The results obtained with the drug combination BMS 1 μ M/AFT 0.25 μ M/XAV 0.25 μ M followed the same profile to the previous condition. Once more, Hep3B cell line (Figure 24B) was the one that presented lower cell viability, 69.97%, after incubation with drug-loaded liposomes, compared to that observed with HepG2 cells (Figure 24A), 103.64%. Free drugs, promoted high cytotoxicity in the two cell lines.

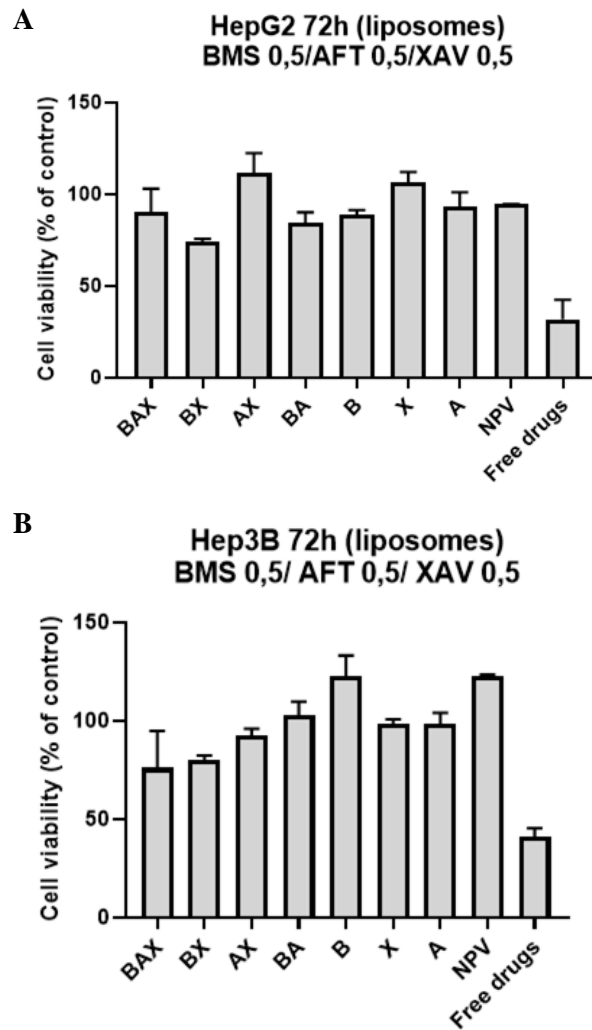


Figure 23. Therapeutic potential of the different liposomes loading the Afatinib, BMS-777607 and XAV-939 drugs and free drugs in BMS 0.5 μ M/ AFT 0.5 μ M/ XAV 0.5 μ M condition combination. HepG2 (**A**) and Hep3B (**B**) cells were treated with the liposomes and free drugs. The cells were incubated for 72h and subsequently viability of the same were analysed using the Alamar blue assay in two independent assays. **NPV** is for empty liposomes, **B** is for BMS-777607 liposome, **A** is for Afatinib liposome and **X** is for XAV-939 liposome.

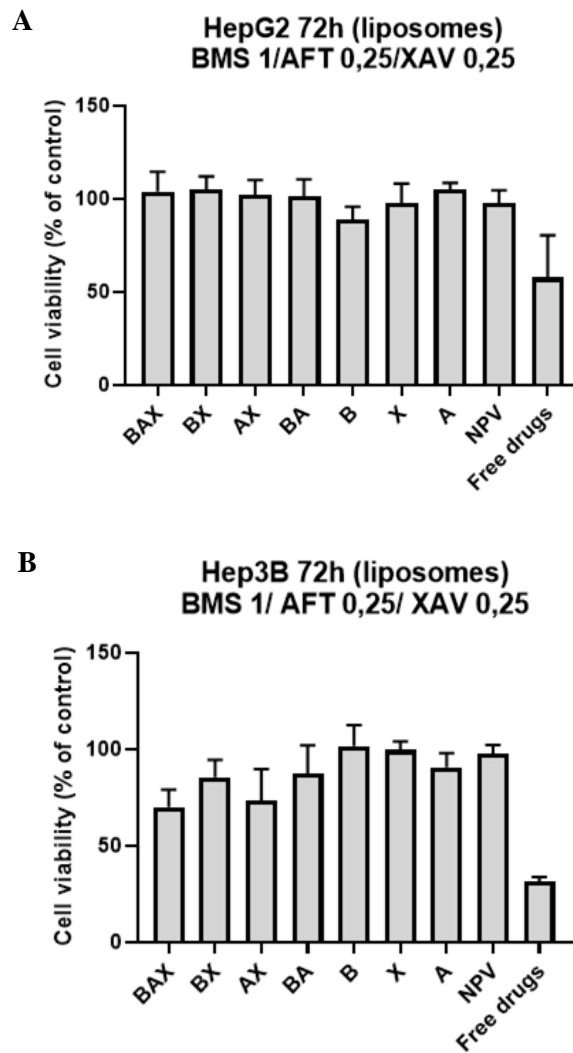


Figure 24. Therapeutic potential of the different liposomes loading the Afatinib, BMS-777607 and XAV-939 drugs and free drugs in BMS 1 μ M/ AFT 0.25 μ M/ XAV 0.25 μ M condition combination. HepG2 (**A**) and Hep3B (**B**) cells were treated with the liposomes and free drugs. The cells were incubated for 72h and subsequently viability of the same were analysed using the Alamar blue assay in two independent assays. **NPV** is for empty liposomes, **B** is for BMS-777607 liposome, **A** is for Afatinib liposome and **X** is for XAV-939 liposome.

4. Discussion

4. Discussion

4.1. Effect of different drug combinations in HCC cell lines

A synergistic effect is a result of two or more processes that interact with each other in order to produce a greater effect than the cumulative effect that those processes produce when used in an isolated form. Combination therapy can be effective and beneficial to a certain purpose in several ways, one of them is by achieving a synergistic effect through this combination.

In this work it was possible to test the different drug combinations between afatinib (AFT), BMS-777607 (BMS) and XAV-939 (XAV) that are responsible for inhibiting some of the major receptors and molecular signaling pathways involved in hepatocellular carcinoma. HCC cells were incubated with different drug combinations and their combination efficacy and synergy in inducing cellular death in HepG2, Hep3B and Huh7 cells was evaluated.

When the drugs were combined it was possible to observe, according to the obtained data (Figure 9, 10, 11 and 12), that several drug combinations resulted in much higher cytotoxicity than that registered with the cumulative effect achieved with the same concentration of the isolated drugs, in the different HCC cell lines. The most outstanding synergistic effect occurred when the three drugs were combined. In these cases, the cells presented very low cellular viability levels. Several drug combinations were able to induce cellular death by 5-fold higher than the sum of the cytotoxicity obtained with the isolated drugs in the same concentrations. The BMS 0.5 μ M/AFT 0.5 μ M/XAV 0.5 μ M drug combination resulted, in HepG2 cells, in a cell viability of 24.63%, and the difference between the sum of cytotoxicity percentages of the isolated drugs and the cytotoxicity of this combination was of 72.62%.

AFT, BMS and XAV are inhibitors of some of the major receptors involved in carcinogenesis, EGFR, c-MET and WNT/ β catenin, respectively (Dai et al., 2012; Dai and Siemann., 2010; Ferrarotto *et al.*, 2013; Li *et al.*, 2008; Lietman *et al.*, 2018; Song *et al.*, 2020) These receptors are overexpressed in HCC cells; therefore, inhibition of apoptosis and an uncontrolled proliferation, angiogenesis, migration and survival of the cells occur. Each receptor is responsible for different tasks in the cell and without the mechanisms that are enumerated above, the tumour won't be able to develop and survive (Dimri *et al.*, 2020; Couri and Pillai., 2019; Robert and Gores., 2005). The receptors activate downstream molecular signaling pathways that might be shared by some of the receptors, which happens with EGFR and c-MET receptors. Both activate PI3K/PIP3/AKT/mTOR and RAS/RAF/MEK/ERK signaling pathways (Dimri *et al.*, 2020). It appears that the combination of the drugs, that inhibit these receptors, results in an effective antitumoral effect. This might be justified by the fact that each drug has the ability to

suppress the activity of different receptors, resulting in a combined inhibition of cellular processes that usually allow the cell to survive and develop. It is possible that the inhibition of two receptors that share the same downstream molecular signaling pathway might result in a greater inhibition of the same (Engelman *et al.*, 2007; Grugan *et al.*, 2017; Moores *et al.*, 2016; Vengoji *et al.*, 2019).

4.1.2. Apoptosis/necrosis of HCC cells treated with the different drug combinations

There are different pathways through which a cell can die, among them are apoptosis and necrosis. Apoptosis is a programmed and regulated process of cell death, it is a passive process with no inflammatory responses and minimal damage to surrounding tissues. Necrosis, on the contrary, is a traumatic and uncontrolled cell death mechanism, causing great injury during its process (D'Arcy., 2019). Given to the fact that apoptosis is a programable cell death with no inflammatory processes, it is preferable that the cells die through apoptosis over necrosis which, as mentioned above, is an inflammatory process of cellular death.

Apoptosis/necrosis assays were performed after a 72h cells incubation with free drug combinations. Combinations of the drugs resulted in a co-staining of Annexin V and Propidium iodide (PI) in the cells. Annexin V staining only, indicates that the cells are undergoing early apoptosis, but when a co-staining of Annexin V and PI is present, cells could be going through late apoptosis or necrosis. A possible justification for the occurrence of this co-staining can be the fact that the cells enter a phase of an early apoptosis which eventually evolve to a late apoptosis phase. In early apoptosis Phosphatidylserine (PS) moves to the outer membrane leaflet allowing the Annexin V to bind to it. In late apoptosis the cellular membrane bursts allowing PI to enter the cells and the same happens with necrotic cells. In order to understand and differentiate late apoptotic cells and necrotic cells, apoptosis/necrosis assays at different incubation times can be performed to monitor Annexin V and PI staining at different times and points of cellular death (Farinha *et al.*, 2021).

During apoptosis, caspase activation event is crucial. Initiator caspases, caspase-9 and caspase-8 are activated by intrinsic and extrinsic pathways, respectively. Initiator caspases lead to the activation of effector caspases, caspase-3 and caspase-7. Effector caspases execute the apoptosis through cleavage of cellular components. Therefore, caspase activity studies might be performed in order to understand if cellular death occurs via apoptosis (Fan *et al.*, 2005; Farinha *et al.*, 2021; Shi., 2002). Furthermore, alteration in the mitochondrial potential through JC-1 probe, can also assist in understanding through which cellular death the cells are going through (Farinha

et al., 2021; Li *et al.*, 2019; Sakthivel *et al.*, 2018). During apoptosis, the morphological changes and degradation of the chromatin occur in late apoptotic stages, thus DNA studies through agarose gel electrophoresis could be the key to differentiate early and late apoptosis (Zhang *et al.*, 1997).

Once more, we can reinforce the synergistic effect of the drug combinations, given that cells incubation with isolated drugs resulted in a reduced stained for Annexin V or PI and presented a high number of living cells, whereas the drug combinations resulted in an elevated Annexin V and PI staining as well as low number of living cells. Therefore, combined drugs tested are more efficient when it comes to cytotoxicity of the HCC cells. The BMS 0.25 μ M/AFT 1 μ M/XAV 0.5 μ M drug combination appears to possess higher efficiency to induce cellular death, since the percentage of live cells in this condition is only 1.06%. Percentage of cells undergoing early apoptosis is higher than the one of necrotic or late apoptotic cells, with 65.13 % of cells in early apoptosis and 33.78 % in a necrotic or late apoptotic phase. Additionally, the cell viability results, obtained with HepG2 cells incubated with the drugs combination BMS 0.25 μ M/AFT 1 μ M/XAV 0.5 μ M, showed 12.84% of cell viability and a notable synergistic effect. Thus, we can infer that this combination holds a great effectiveness in inducing cellular death to hepatocellular carcinoma cells.

4.2. Production of hybrid nanosystems and encapsulation of the drugs

Administration of isolated drugs might result in undesirable secondary effects, that reflect in the patient's quality of life. Nanotechnology has been widely used in nanomedicine and has shown to possess a variety of qualities and advantages (Jong and Borm., 2008; Seaberg *et al.*, 2021). Production of nanosystems with different nanomaterials can result in a more stable and efficient nanocarrier, with superior features that combined advantages of each material (Ferreira Soares *et al.*, 2020). Some of the major advantages of these nanosystems are specific delivery to the target and thus a lower occurrence of undesirable secondary effects, protection of the therapeutic agents and their leakage during their delivery (Jong and Borm., 2008; Seaberg *et al.*, 2021). Hybrid lipid-polymer nanosystems result in merged benefits when the two compounds, lipids and polymers, are combined. Liposomes are highly biocompatible as they are composed of lipidic bilayer and polymers possess structural integrity that liposomes are in lack of, therefore polymers confer higher stability to the nanosystems. Thus, hybrid lipid-polymer nanosystems originate a biocompatible and stable nanosystems with the capacity of encapsulating different therapeutic agents and delivering them to the target avoiding leakage and degradation of the same and decreasing secondary effects (Cheow and Hadinoto., 2011).

In this part of the work, an optimization of PLGA nanoparticles using a sonication probe was accomplished. Different times and amplitude of sonication as well as PLGA percentages were tested to reach an optimal size of the nanoparticles, which to our objective was around 120 nm. The purpose of these nanoparticles is to be administered via intravenously, therefore their size should comply with the parameters to this end. The capacity of encapsulation of the nanoparticles is proportional to their size, the bigger the nanoparticle, the bigger the capacity of its encapsulation. A nanoparticle with 120 nm is capable of reaching high percentages of drug encapsulation.

It was observed that there is a small tendency to increase PLGA nanoparticles size as the amplitude percentage of sonication decreases and the same happened with the time of the sonication, shorter time of sonication resulted in slightly bigger nanoparticles. Even though the alteration of these parameters might be correlated with nanoparticles size, these differences don't appear to have a statistical significance. A slightly more notable size difference was observed when PLGA percentage was increased, PLGA 3% resulted in bigger nanoparticles when compared to PLGA 2%. A possible justification to the obtained results is that a higher sonication amplitude and longer sonication time might provoke a better homogenization of the nanoparticles resulting in their smaller size (Shi *et al.*, 2011; Das *et al.*, 2011).

With this, after several conditions evaluated and characterizations performed, we chose the condition 1 minute of sonication with a 50% of amplitude and PLGA 3% to encapsulate the drugs. The nanoparticles size was of 118.6 ± 0.36 nm with a PI (polydispersity index) of 0.060 ± 0.012 , which is a good size to proceed with the drug encapsulation, and 0.012 is under 0.2, which means that the produced nanoparticles are not polydisperse.

As a subsequent task, the drugs were encapsulated in the PLGA nanoparticles. The size of the nanoparticles was around 115-125nm, which should allow a high encapsulation of the drugs. When the drugs were encapsulated in the PLGA nanoparticles, the loading efficiency of AFT and XAV were low and only BMS presented a high percentage loading efficiency, 67.9%, and high loading capacity, $19.53\mu\text{g}$ of drug/mg of NP. This could be justified by the fact that the three drugs present a different molecule structure, size, polarity and hydrophobicity, which could lead to their different interaction with the nanoparticles and therefore, dissimilar loading capacity (Leonetti *et al.*, 2021; Das *et al.*, 2011).

In an attempt to avoid the low encapsulation issue with AFT and XAV drugs, these were posteriorly encapsulated in the liposomes, 0.2 mg of each drug per 5.34 mg of lipids. Liposomes and PLGA nanoparticles possess different physicochemical properties, hence different hydrophobic environments that allow the encapsulation of these two drugs in the liposomes. As the liposomes were produced, hybrid nanosystems were created through the mixture of PLGA nanoparticle and liposome. This resulted in a hybrid nanosystem loaded with therapeutic agents that will be specifically delivered to the hepatocellular carcinoma cells, due to the GalNAc ligand

present in the lipidic bilayer of the liposomes that binds specifically to the ASGP receptors (Ivanenkov *et al.*, 2018).

Two of the promising conditions tested with free drugs were chosen to be tested in hybrid nanosystems (BMS 0,5 μ M/AFT 0,5 μ M/XAV 0,5 μ M and BMS 1 μ M/AFT 0,25 μ M/XAV 0,25 μ M), but overall hybrid nanosystems didn't quite fulfil the task of dropping the HCC cells viability levels as free drugs did, even so, these results should not be discharged as these might be promising. These results can be justified by the incapacity of the nanosystems to release the drugs or to the drug degradation over time or during the nanosystem production process. The production of PLGA nanoparticles includes a process of sonication that might be causing drugs' degradation, temperature and light might also perturb the drugs' stability. The incubation and mixture of the PLGA nanoparticles with liposomes require high temperature that can lead to an alteration of the drugs' efficacy. Further studies must be carried out, such as release assays, to determine the reason behind these results.

In summary, the cell viability levels registered when these were incubated with hybrid nanosystems encapsulating the drugs, for both drug combinations, were higher than that observed with the free drug combinations, which means that the drugs that were encapsulated in the nanosystems did not effectively interfere with the HCC cells. On the other hand, Hep3B cell line presented a significant decrease in cell viability levels with BMS 1 μ M/AFT 0,25 μ M/XAV 0,25 μ M condition and HepG2 also had a slight drop in cell viability with BMS 0,5 μ M/AFT 0,5 μ M/XAV 0,5 μ M condition. Therefore, forward studies should be performed in order to analyse the potential of hybrid nanosystems encapsulating drugs to induce cellular death to HCC cells which might be promising. Nevertheless, obtained results led us to consider the development of another drug delivery formulation.

4.3. Production of Asialofetuin-coated PLGA nanoparticles loaded with BMS-777607

As asialofetuin (ASF) is a specific ligand of the ASGP (asialoglycoprotein) (Thapa *et al.*, 2015) receptors and BMS drug exhibited high encapsulation in PLGA nanoparticles, a new formulation of ASF-coated PLGA nanoparticles with encapsulated BMS was developed, and its efficacy to induce HCC cells death was evaluated. DMAB surfactant was added to nanoparticles to create a positive surface charge and thus allowing the establishment of electrostatic interaction with the negatively charged ASF. As described in the results section, different ASF concentrations were tested, therefore, nanoparticles with different asialofetuin concentrations, ranging from 0 to 150 μ g ASF/mg NP, were produced. Nanoparticles were loaded with a fluorescent probe,

coumarin-6, and internalization assays were carried out to confirm if the nanoparticles enter the cells.

After the conclusion of the cellular internalization assays, we confirmed, indeed, that the nanoparticles were internalized by the cells. Although in all conditions an internalization occurred, we chose 125 $\mu\text{g ASF/mg NP}$ condition to further studies, since it presented a slightly higher Geo Mean value, which mean a higher cellular internalization. After the addition of ASF (in 125 $\mu\text{g ASF/mg NP}$ concentration) to the positively charged nanoparticles, 19.9 mV, their zeta potential became negative, -9.02mV, and the size of the nanoparticles rose from 94.78nm to 113.5nm. With these results we can assume that the PLGA nanoparticles were successfully coated with ASF. Another possible reason for the nanoparticles size differences might be related with the production process, that was slightly altered in this case. Ultraturrax Homogenizer was used instead of the sonication probe.

Additionally, we believe that a specific binding between nanoparticles and cells occur. In the absence of ASF, 0 $\mu\text{g ASF/mg NP}$, the cellular internalization of the nanoparticles occurred through an unspecific binding, given that the cells surface charge is negative and the zeta potential of these nanoparticles is positive, giving rise to an electrostatic interaction. Nevertheless, when nanoparticles were coated with ASF, 125 $\mu\text{g ASF/mg NP}$, the internalization of the nanoparticles still occurred, even though zeta potential of these nanoparticles is negative and electrostatic repulsion between the cells and nanoparticles is expected to occur. Hence, this could be an indication of a specific interaction between the nanoparticles and the ASGPR at the cells surface, promoting the cell uptake of the nanoparticles. To analyse this hypothesis, an assay of competitive inhibition of the ASGP receptors could be performed, in order to confirm if the internalization of the nanoparticles is mediated by the specific interaction of the ASF with ASGPR.

An encapsulation of BMS-7777607 drug was conducted and later on, the nanoparticles were coated with ASF and HepG2 cells were incubated with empty and BMS-loaded nanoparticles. Alamar Blue assay demonstrated that there is a slight difference between the cell viability levels when it comes to nanoparticles concentrations, higher concentrations induce more cytotoxicity. Cell viability decrease occurred after incubation with BMS-loaded nanoparticles. Nevertheless, empty nanoparticles also presented cytotoxicity, possibly due to the presence of the extra surfactant in the nanoparticles formulation that promote the cells membrane rupture and induce cellular toxicity. However, BMS-loaded nanoparticles induced a higher cytotoxicity than empty nanoparticles, showing antitumor effect promoted by the drug release from the nanoparticles.

4.4. Production of liposomes loaded with afatinib, BMS-777607 and XAV-939

Since liposomes have a great potential as a nanocarrier and we observed a great synergistic effect with the AFT, BMS and XAV combination, we encapsulated the drugs in the liposomes. Once again, first, we wanted to make sure that the liposomes were internalized by the HCC cells, hence, the liposomes were loaded with coumarin-6 and internalization assays were carried out. As soon as we confirmed that the uptake of the liposomes by the cells occurred, we moved on to the encapsulation of the drugs and incubations with the HCC cells.

Liposomes contained the GalNAc ligand, at the surface of the lipid bilayer, that promoted their specific binding to the HCC cells through the ASGP receptors (Prakash *et al.*, 2014). Internalization assays results demonstrated that the cellular internalization of liposomes was directly proportional to their concentration, given that higher liposome concentrations resulted in higher Geo Mean levels and as this concentration decrease so does the Geo Mean value. Subsequently, HepG2 and Hep3B cells were incubated with the drug-loaded liposomes, having been observed a significant decrease in the cell viability of Hep3B cells with the BMS 0.5 μ M/ AFT 0.5 μ M/ XAV 0.5 μ M and BMS 1 μ M/ AFT 0.25 μ M/ XAV 0.25 μ M drug combinations. Possibly, to understand these results and to achieve greater ones, different concentrations of the liposomes should be tested.

5. Conclusion

5. Conclusion

Concluding from the results obtained in this dissertation, there is great antitumor potential when it comes to the combinations of the drugs, given that a variety of combinations that were tested resulted in a great decrease of cell viability when compared to cell viability levels when the cells were treated with individual drugs. The best results were achieved when the three drugs, afatinib, BMS-777607 and XAV-939, were combined. The combinations BMS 0,5 μ M/ AFT 0,5 μ M/ XAV 0,5 μ M; BMS 1 μ M/ AFT 0,25 μ M/ XAV 0,25 μ M and BMS 0,25 μ M/ AFT 1 μ M/ XAV 0,5 μ M were some of the best combinations, that induced high cytotoxicity to HCCC cells and presented with notable synergistic effect. Further, apoptosis/necrosis studies have reinforced the potential of these combinations to induce cytotoxicity to the HepG2 cells. It was observed that when the cells were treated with these combinations, a significant cellular death occurred, most likely, through apoptosis. Thus, these combinations hold a great synergistic effect when it comes to antitumoral strategy to HCC.

Furthermore, a reduced cell viability was observed in HepG2 cells when these were incubated with hybrid nanosystems encapsulating the BMS 0.5 μ M/AFT 0.5 μ M/XAV 0.5 μ M drug combination. Hep3B cell viability was also decreased when treated with hybrid nanosystems encapsulating the BMS 1 μ M/AFT 0.25 μ M/XAV 0.25 μ M drug combination. When it comes to liposomes encapsulating afatinib, BMS-777607 and XAV-939, with the same conditions as in hybrid nanosystems BMS 0.5 μ M/AFT 0.5 μ M/XAV 0.5 μ M and BMS 1 μ M/AFT 0.25 μ M/XAV 0.25 μ M, these combinations induced higher cytotoxicity in Hep3B cell line. Although these results are not as outshining as those obtained with free drug combinations, they are still promising, since nanosystems can overcome some of the limitations associated to free drug administration. The drug combination alongside with the nanosystem formulation, might bring a powerful tool to fight this disease. As mentioned before thought this dissertation, the hybrid nanosystem formulation holds various positive features. These nanosystems are small and thus it is possible to perform an intravenous administration of the same to the patient. The nanosystems are biocompatible and biodegradable, that deliver the drugs directly to their target, avoiding secondary effects that free drugs often cause.

As to ASF-coated PLGA nanoparticles encapsulating the BMS-777607 drug, a decrease in the viability of the cells was also observed, as incubation with empty nanoparticles resulted in higher cell viability percentages when compared to cells treated with nanoparticles encapsulating the drug. The cytotoxicity of NPs could have been affected by the presence of extra surfactant, DMAB, in their formulation, nevertheless, nanosystems with BMS-777607 still resulted in lower cell viability percentages, showing their antitumor effect. Conclusively, some of the data obtained

in this work might hold great potential to HCC treatment, and therefore further studies should be performed in order to better understand these results and improve the developed formulations.

6. References

6. References

- Alexia, C., Fallot, G., Lasfer, M., Schweizer-Groyer, G., & Groyer, A. (2004). An evaluation of the role of insulin-like growth factors (IGF) and of type-I IGF receptor signalling in hepatocarcinogenesis and in the resistance of hepatocarcinoma cells against drug-induced apoptosis. In *Biochemical Pharmacology* (Vol. 68, pp. 1003–1015).
- Almasoud, N., Binhamdan, S., Younis, G., Alaskar, H., Alotaibi, A., Manikandan, M., ... AlMuraikhi, N. (2020). Tankyrase inhibitor XAV-939 enhances osteoblastogenesis and mineralization of human skeletal (mesenchymal) stem cells. *Scientific Reports*, *10*(1).
- Alqahtani, A., Khan, Z., Alloghbi, A., Ahmed, T. S. S., Ashraf, M., & Hammouda, D. M. (2019, September 1). Hepatocellular carcinoma: Molecular mechanisms and targeted therapies. *Medicina (Lithuania)*. MDPI AG.
- Apte, U., Thompson, M. D., Cui, S., Liu, B., Cieply, B., & Monga, S. P. S. (2008). Wnt/ β -catenin signaling mediates oval cell response in rodents. *Hepatology*, *47*(1), 288–295.
- Avila, M. A., Berasain, C., Sangro, B., & Prieto, J. (2006, June 26). New therapies for hepatocellular carcinoma. *Oncogene*.
- Azevedo, A., Farinha, D., Geraldés, C., & Faneca, H. (2021, September 5). Combining gene therapy with other therapeutic strategies and imaging agents for cancer theranostics. *International Journal of Pharmaceutics*. Elsevier B.V.
- Bider, M. D., & Spiess, M. (1998). Ligand-induced endocytosis of the asialoglycoprotein receptor: Evidence for heterogeneity in subunit oligomerization. *FEBS Letters*, *434*(1–2), 37–41.
- Bregoli, L., Movia, D., Gavigan-Imedio, J. D., Lysaght, J., Reynolds, J., & Prina-Mello, A. (2016, January 1). Nanomedicine applied to translational oncology: A future perspective on cancer treatment. *Nanomedicine: Nanotechnology, Biology, and Medicine*. Elsevier Inc.
- Brunetti, O., Gnoni, A., Licchetta, A., Longo, V., Calabrese, A., Argentiero, A., ... Silvestris, N. (2019, October 1). Predictive and prognostic factors in HCC patients treated with sorafenib. *Medicina (Lithuania)*. MDPI AG.

Chaturvedi, V. K., Singh, A., Singh, V. K., & Singh, M. P. (2018). Cancer Nanotechnology: A New Revolution for Cancer Diagnosis and Therapy. *Current Drug Metabolism*, 20(6), 416–429.

Cheow, W. S., & Hadinoto, K. (2011). Factors affecting drug encapsulation and stability of lipid-polymer hybrid nanoparticles. *Colloids and Surfaces B: Biointerfaces*, 85(2), 214–220.

Couri, T., & Pillai, A. (2019, March 12). Goals and targets for personalized therapy for HCC. *Hepatology International*. Springer.

Dai, Y., Bae, K., Pampo, C., & Siemann, D. W. (2012). Impact of the small molecule Met inhibitor BMS-777607 on the metastatic process in a rodent tumor model with constitutive c-Met activation. *Clinical and Experimental Metastasis*, 29(3), 253–261.

Dai, Y., & Siemann, D. W. (2010). BMS-777607, a small-molecule Met kinase inhibitor, suppresses hepatocyte growth factor-stimulated prostate cancer metastatic phenotype in vitro. *Molecular Cancer Therapeutics*, 9(6), 1554–1561.

Danhier, F., Ansorena, E., Silva, J. M., Coco, R., Le Breton, A., & Pr eat, V. (2012, July 20). PLGA-based nanoparticles: An overview of biomedical applications. *Journal of Controlled Release*.

D'Arcy, M. S. (2019, June 1). Cell death: a review of the major forms of apoptosis, necrosis and autophagy. *Cell Biology International*. Wiley-Blackwell Publishing Ltd.

Das, S., Ng, W. K., Kanaujia, P., Kim, S., & Tan, R. B. H. (2011). Formulation design, preparation and physicochemical characterizations of solid lipid nanoparticles containing a hydrophobic drug: Effects of process variables. *Colloids and Surfaces B: Biointerfaces*, 88(1), 483–489.

Date, T., Nimbalkar, V., Kamat, J., Mittal, A., Mahato, R. I., & Chitkara, D. (2018, February 10). Lipid-polymer hybrid nanocarriers for delivering cancer therapeutics. *Journal of Controlled Release*. Elsevier B.V.

Detampel, P., Witzigmann, D., Kr ahenb uhl, S., & Huwyler, J. (2014). Hepatocyte targeting using pegylated asialofetuin-conjugated liposomes. *Journal of Drug Targeting*, 22(3), 232–241.

Dimri, M., & Satyanarayana, A. (2020, February 1). Molecular signaling pathways and therapeutic targets in hepatocellular carcinoma. *Cancers*. MDPI AG.

Dittfeld, C., Reimann, G., Mieting, A., Büttner, P., Jannasch, A., Plötze, K., ... Matschke, K. (2018). Treatment with XAV-939 prevents in vitro calcification of human valvular interstitial cells. *PLoS ONE*, 13(12).

Ding, D., & Zhu, Q. (2018, November 1). Recent advances of PLGA micro/nanoparticles for the delivery of biomacromolecular therapeutics. *Materials Science and Engineering C*. Elsevier Ltd.

Engelman, J. A., Zejnullahu, K., Mitsudomi, T., Song, Y., Hyland, C., Joon, O. P., ... Jänne, P. A. (2007). MET amplification leads to gefitinib resistance in lung cancer by activating ERBB3 signaling. *Science*, 316(5827), 1039–1043.

Fan, T. J., Han, L. H., Cong, R. S., & Liang, J. (2005). Caspase family proteases and apoptosis. *Acta Biochimica et Biophysica Sinica*, 37(11), 719–727.

Farinha, D., Migawa, M., Sarmiento-Ribeiro, A., & Faneca, H. (2021). A combined antitumor strategy mediated by a new targeted nanosystem to hepatocellular carcinoma. *International Journal of Nanomedicine*, 16, 3385–3405.

Farinha, D., Pedroso De Lima, M. C., & Faneca, H. (2014). Specific and efficient gene delivery mediated by an asialofetuin-associated nanosystem. *International Journal of Pharmaceutics*, 473(1–2), 366–374.

Farokhzad, O. C., & Langer, R. (2009). Impact of Nanotechnology on Hair Attributes. *ACS Nano*, 3(1), 1–7.

Ferreira Soares, D. C., Domingues, S. C., Viana, D. B., & Tebaldi, M. L. (2020, November 1). Polymer-hybrid nanoparticles: Current advances in biomedical applications. *Biomedicine and Pharmacotherapy*. Elsevier Masson SAS.

Ferrarotto, R., & Gold, K. A. (2014). Afatinib in the treatment of head and neck squamous cell carcinoma. *Expert Opinion on Investigational Drugs*, 23(1), 135–143.

Fouladi, F., Steffen, K. J., & Mallik, S. (2017). Enzyme-Responsive Liposomes for the Delivery of Anticancer Drugs. *Bioconjugate Chemistry*, 28(4), 857–868.

Fujiwara, N., Friedman, S. L., Goossens, N., & Hoshida, Y. (2018, March 1). Risk factors and prevention of hepatocellular carcinoma in the era of precision medicine. *Journal of Hepatology*. Elsevier B.V.

Galuppo, R., Ramaiah, D., Ponte, O. M., & Gedaly, R. (2014). Molecular therapies in hepatocellular carcinoma: What can we target? *Digestive Diseases and Sciences*. Springer New York LLC.

Geffen, I., & Spiess, M. (1993). Asialoglycoprotein Receptor. *International Review of Cytology*, 137, 181–219.

Gentile, P., Chiono, V., Carmagnola, I., & Hatton, P. V. (2014, February 28). An overview of poly(lactic-co-glycolic) Acid (PLGA)-based biomaterials for bone tissue engineering. *International Journal of Molecular Sciences*. Molecular Diversity Preservation International.

Grugan, K. D., Dorn, K., Jarantow, S. W., Bushey, B. S., Pardinias, J. R., Laquerre, S., ... Chiu, M. L. (2017). Fc-mediated activity of EGFR x c-Met bispecific antibody JNJ-61186372 enhanced killing of lung cancer cells. *MAbs*, 9(1), 114–126.

Hadinoto, K., Sundaresan, A., & Cheow, W. S. (2013). Lipid-polymer hybrid nanoparticles as a new generation therapeutic delivery platform: A review. *European Journal of Pharmaceutics and Biopharmaceutics*. Elsevier B.V.

Harvey, R. D., Adams, V. R., Beardslee, T., & Medina, P. (2020, September 1). Afatinib for the treatment of EGFR mutation-positive NSCLC: A review of clinical findings. *Journal of Oncology Pharmacy Practice*. SAGE Publications Ltd.

Hartke, J., Johnson, M., & Ghabril, M. (2017). The diagnosis and treatment of hepatocellular carcinoma. *Seminars in Diagnostic Pathology*, 34(2), 153–159.

Hossen, S., Hossain, M. K., Basher, M. K., Mia, M. N. H., Rahman, M. T., & Uddin, M. J. (2019, January 1). Smart nanocarrier-based drug delivery systems for cancer therapy and toxicity studies: A review. *Journal of Advanced Research*. Elsevier B.V.

Huang, S. M. A., Mishina, Y. M., Liu, S., Cheung, A., Stegmeier, F., Michaud, G. A., ... Cong, F. (2009). Tankyrase inhibition stabilizes axin and antagonizes Wnt signalling. *Nature*, 461(7264), 614–620.

Igdoura, S. A. (2017, April 1). Asialoglycoprotein receptors as important mediators of plasma lipids and atherosclerosis. *Current Opinion in Lipidology*. Lippincott Williams and Wilkins.

Ivanenkov, Y. A., Majouga, A. G., Petrov, R. A., Petrov, S. A., Kovalev, S. V., Maklakova, S. Y., ... Beloglazkina, E. K. (2018). Synthesis and biological evaluation of novel doxorubicin-

containing ASGP-R-targeted drug-conjugates. *Bioorganic and Medicinal Chemistry Letters*, 28(3), 503–508.

Jindal, A., Thadi, A., & Shailubhai, K. (2019, March 1). Hepatocellular Carcinoma: Etiology and Current and Future Drugs. *Journal of Clinical and Experimental Hepatology*. Elsevier B.V.

Jong, W. H. D., & Paul, J. B. (2008). Drug delivery and nanoparticles : Applications and hazards. *International Journal of Nanomedicine*, 3(2), 133–149.

Khorev, O., Stokmaier, D., Schwardt, O., Cutting, B., & Ernst, B. (2008). Trivalent, Gal/GalNAc-containing ligands designed for the asialoglycoprotein receptor. *Bioorganic and Medicinal Chemistry*, 16(9), 5216–5231.

Kulik, L., & El-Serag, H. B. (2019). Epidemiology and Management of Hepatocellular Carcinoma. *Gastroenterology*, 156(2), 477-491.e1.

Leonetti, B., Perin, A., Ambrosi, E. K., Sponchia, G., Sgarbossa, P., Castellin, A., ... Scarso, A. (2021). Mesoporous zirconia nanoparticles as drug delivery systems: Drug loading, stability and release. *Journal of Drug Delivery Science and Technology*, 61.

Li, D., Ambrogio, L., Shimamura, T., Kubo, S., Takahashi, M., Chirieac, L. R., ... Wong, K. K. (2008). BIBW2992, an irreversible EGFR/HER2 inhibitor highly effective in preclinical lung cancer models. *Oncogene*, 27(34), 4702–4711.

Li, M., Du, C., Guo, N., Teng, Y., Meng, X., Sun, H., ... Galons, H. (2019, February 15). Composition design and medical application of liposomes. *European Journal of Medicinal Chemistry*. Elsevier Masson s.r.l.

Li, Y., Wu, Q., Yu, G., Li, L., Zhao, X., Huang, X., & Mei, W. (2019). Polypyridyl Ruthenium(II) complex-induced mitochondrial membrane potential dissipation activates DNA damage-mediated apoptosis to inhibit liver cancer. *European Journal of Medicinal Chemistry*, 164, 282–291.

Lietman, C., Wu, B., Lechner, S., Shinar, A., Sehgal, M., Rossomacha, E., ... Young, P. P. (2018). Inhibition of Wnt/ β -catenin signaling ameliorates osteoarthritis in a murine model of experimental osteoarthritis. *JCI Insight*, 3(3).

Liu, Y., Xie, X., Chen, H., Hou, X., He, Y., Shen, J., ... Feng, N. (2020, October 1). Advances in next-generation lipid-polymer hybrid nanocarriers with emphasis on polymer-modified

functional liposomes and cell-based-biomimetic nanocarriers for active ingredients and fractions from Chinese medicine delivery. *Nanomedicine: Nanotechnology, Biology, and Medicine*. Elsevier Inc.

Matsumoto, K., & Nakamura, T. (1996). Emerging multipotent aspects of hepatocyte growth factor. *Journal of Biochemistry*. Oxford University Press.

Mc Carthy, D. J., Malhotra, M., O'Mahony, A. M., Cryan, J. F., & O'Driscoll, C. M. (2015). Nanoparticles and the blood-brain barrier: Advancing from in-vitro models towards therapeutic significance. *Pharmaceutical Research*, 32(4), 1161–1185.

Moores, S. L., Chiu, M. L., Bushey, B. S., Chevalier, K., Luistro, L., Dorn, K., ... Anderson, G. M. (2016). A novel bispecific antibody targeting EGFR and cMet is effective against EGFR inhibitor-resistant lung tumors. *Cancer Research*, 76(13), 3942–3953.

Mukherjee, P., Khademhosseini, A., Seaberg, J., Montazerian, H., Hossen, M. N., & Bhattacharya, R. (2021, February 23). Hybrid nanosystems for biomedical applications. *ACS Nano*. American Chemical Society.

Muto, J., Shirabe, K., Sugimachi, K., & Maehara, Y. (2015, January 1). Review of angiogenesis in hepatocellular carcinoma. *Hepatology Research*. Blackwell Publishing Ltd.

Nigam, K., Kaur, A., Tyagi, A., Nematullah, M., Khan, F., Gabrani, R., & Dang, S. (2019). Nose-to-brain delivery of lamotrigine-loaded PLGA nanoparticles. *Drug Delivery and Translational Research*, 9(5), 879–890.

Nair, J. K., Willoughby, J. L. S., Chan, A., Charisse, K., Alam, M. R., Wang, Q., ... Manoharan, M. (2014). Multivalent N -acetylgalactosamine-conjugated siRNA localizes in hepatocytes and elicits robust RNAi-mediated gene silencing. *Journal of the American Chemical Society*, 136(49), 16958–16961.

Peer, D., Karp, J. M., Hong, S., Farokhzad, O. C., Margalit, R., & Langer, R. (2007, December). Nanocarriers as an emerging platform for cancer therapy. *Nature Nanotechnology*.

Peetla, C., Jin, S., Weimer, J., Elegbede, A., & Labhasetwar, V. (2014). Biomechanics and thermodynamics of nanoparticle interactions with plasma and endosomal membrane lipids in cellular uptake and endosomal escape. *Langmuir*, 30(25), 7522–7532.

Pinto Marques, H., Gomes da Silva, S., De Martin, E., Agopian, V. G., & Martins, P. N. (2020, October 1). Emerging biomarkers in HCC patients: Current status. *International Journal of Surgery*. Elsevier Ltd.

Prakash, T. P., Graham, M. J., Yu, J., Carty, R., Low, A., Chappell, A., ... Seth, P. P. (2014). Targeted delivery of antisense oligonucleotides to hepatocytes using triantennary N-acetyl galactosamine improves potency 10-fold in mice. *Nucleic Acids Research*, *42*(13), 8796–8807.

Rezvantalab, S., Drude, N. I., Moraveji, M. K., Güvener, N., Koons, E. K., Shi, Y., ... Kiessling, F. (2018). PLGA-based nanoparticles in cancer treatment. *Frontiers in Pharmacology*, *9*(NOV).

Roberts, L. R., & Gores, G. J. (2005, May). Hepatocellular carcinoma: Molecular pathways and new therapeutic targets. *Seminars in Liver Disease*.

Sakthivel, R., Malar, D. S., & Devi, K. P. (2018). Phytol shows anti-angiogenic activity and induces apoptosis in A549 cells by depolarizing the mitochondrial membrane potential. *Biomedicine and Pharmacotherapy*, *105*, 742–752.

Semela, D., & Dufour, J. F. (2004, November). Angiogenesis and hepatocellular carcinoma. *Journal of Hepatology*.

Shah, S., Dhawan, V., Holm, R., Nagarsenker, M. S., & Perrie, Y. (2020, January 1). Liposomes: Advancements and innovation in the manufacturing process. *Advanced Drug Delivery Reviews*. Elsevier B.V.

Sharma, S., Zeng, J. Y., Zhuang, C. M., Zhou, Y. Q., Yao, H. P., Hu, X., ... Wang, M. H. (2013). Small-molecule inhibitor BMS-777607 induces breast cancer cell polyploidy with increased resistance to cytotoxic chemotherapy agents. *Molecular Cancer Therapeutics*, *12*(5), 725–736.

Shi, A. M., Li, D., Wang, L. J., Li, B. Z., & Adhikari, B. (2011). Preparation of starch-based nanoparticles through high-pressure homogenization and miniemulsion cross-linking: Influence of various process parameters on particle size and stability. *Carbohydrate Polymers*, *83*(4), 1604–1610.

Shi, Y. (2002). Mechanisms of caspase activation and inhibition during apoptosis. *Molecular Cell*. Cell Press.

Siepmann, J., Faham, A., Clas, S. D., Boyd, B. J., Jannin, V., Bernkop-Schnürch, A., ... Leroux, J. C. (2019, March 10). Lipids and polymers in pharmaceutical technology: Lifelong companions. *International Journal of Pharmaceutics*. Elsevier B.V.

- Song, S., Huang, H., Guan, X., Fiesler, V., Bhuiyan, M. I. H., Liu, R., ... Begum, G. (2021). Activation of endothelial Wnt/ β -catenin signaling by protective astrocytes repairs BBB damage in ischemic stroke. *Progress in Neurobiology*, 199.
- Tang, W., Chen, Z., Zhang, W., Cheng, Y., Zhang, B., Wu, F., ... Wang, X. (2020, December 1). The mechanisms of sorafenib resistance in hepatocellular carcinoma: theoretical basis and therapeutic aspects. *Signal Transduction and Targeted Therapy*. Springer Nature.
- Thapa, B., Kumar, P., Zeng, H., & Narain, R. (2015). Asialoglycoprotein receptor-mediated gene delivery to hepatocytes using galactosylated polymers. *Biomacromolecules*, 16(9), 3008–3020.
- Torchilin, V. (2009, March). Multifunctional and stimuli-sensitive pharmaceutical nanocarriers. *European Journal of Pharmaceutics and Biopharmaceutics*.
- Tran, S., DeGiovanni, P., Piel, B., & Rai, P. (2017). Cancer nanomedicine: a review of recent success in drug delivery. *Clinical and Translational Medicine*, 6(1).
- Trerè, D., Fiume, L., De Giorgi, L. B., Di Stefano, G., Migaldi, M., & Derenzini, M. (1999). The asialoglycoprotein receptor in human hepatocellular carcinomas: Its expression on proliferating cells. *British Journal of Cancer*, 81(3), 404–408.
- Troutier, A. L., Delair, T., Pichot, C., & Ladavière, C. (2005). Physicochemical and interfacial investigation of lipid/polymer particle assemblies. *Langmuir*, 21(4), 1305–1313.
- Ueki, T., Fujimoto, J., Suzuki, T., Yamamoto, H., & Okamoto, E. (1997). Expression of hepatocyte growth factor and its receptor, the c-met proto-oncogene, in hepatocellular carcinoma. *Hepatology*, 25(3), 619–623.
- Vengoji, R., Macha, M. A., Nimmakayala, R. K., Rachagani, S., Siddiqui, J. A., Mallya, K., ... Shonka, N. (2019). Afatinib and Temozolomide combination inhibits tumorigenesis by targeting EGFRvIII-cMet signaling in glioblastoma cells. *Journal of Experimental and Clinical Cancer Research*, 38(1).
- Wang, Y., You, W., & Li, X. (2020). Current status of gene therapy in melanoma treatment. *Biocell*, 44(2), 167–174.
- Wecker, H., & Waller, C. F. (2018). Afatinib. *Small Molecules in Oncology*, 199–215.

Whittaker, S., Marais, R., & Zhu, A. X. (2010). The role of signaling pathways in the development and treatment of hepatocellular carcinoma. *Oncogene*, 29(36), 4989–5005.

Wicki, A., Witzigmann, D., Balasubramanian, V., & Huwyler, J. (2015, February 28). Nanomedicine in cancer therapy: Challenges, opportunities, and clinical applications. *Journal of Controlled Release*. Elsevier B.V.

Wolfram, J., & Ferrari, M. (2019, April 1). Clinical cancer nanomedicine. *Nano Today*. Elsevier B.V.

Wu, C. C., Weng, C. S., Hsu, Y. T., & Chang, C. L. (2019). Antitumor effects of BMS-777607 on ovarian cancer cells with constitutively activated c-MET. *Taiwanese Journal of Obstetrics and Gynecology*, 58(1), 145–152.

Wu, J., Liu, P., Zhu, J. L., Maddukuri, S., & Zern, M. A. (1998). Increased liver uptake of liposomes and improved targeting efficacy by labeling with asialofetuin in rodents. *Hepatology*, 27(3), 772–778.

Xu, X., Lai, Y., & Hua, Z. C. (2019, January 18). Apoptosis and apoptotic body: Disease message and therapeutic target potentials. *Bioscience Reports*. Portland Press Ltd.

Yang, J. D., Hainaut, P., Gores, G. J., Amadou, A., Plymoth, A., & Roberts, L. R. (2019, October 1). A global view of hepatocellular carcinoma: trends, risk, prevention and management. *Nature Reviews Gastroenterology and Hepatology*. Nature Publishing Group.

Yuan, R., Hou, Y., Sun, W., Yu, J., Liu, X., Niu, Y., ... Chen, X. (2017). Natural products to prevent drug resistance in cancer chemotherapy: a review. *Annals of the New York Academy of Sciences*. Blackwell Publishing Inc.

Zhang, B. C., Luo, B. Y., Zou, J. J., Wu, P. Y., Jiang, J. L., Le, J. Q., ... Shao, J. W. (2020). Co-delivery of Sorafenib and CRISPR/Cas9 Based on Targeted Core-Shell Hollow Mesoporous Organosilica Nanoparticles for Synergistic HCC Therapy. *ACS Applied Materials and Interfaces*, 12(51), 57362–57372.

Zhang, G., Gurtu, V., Kain, S. R., & Yan, G. (1997). Annexin V-FITC Binding Assay. *BioTechniques*, 25(September), 525–531.

Zhang, Q. Y., Wang, F. X., Jia, K. K., & Kong, L. D. (2018). Natural product interventions for chemotherapy and radiotherapy-induced side effects. *Frontiers in Pharmacology*, 9(NOV)